

## Supporting Information

# Highly Luminescent 2-Phenylpyridine-Free Diiridium Complexes with Bulky 1,2-Diarylimidazole Cyclometalating Ligands

Daniel G. Congrave\* Andrei S. Batsanov and Martin R. Bryce\*

*Department of Chemistry, Durham University, Durham DH1 3LE, U.K.*

Email: [m.r.bryce@durham.ac.uk](mailto:m.r.bryce@durham.ac.uk)

<b>Contents</b>	<b>Page</b>
Experimental Section	S2
Copies of NMR Spectra	S9
Electrochemistry	S39
Photophysics	S40
Computations	S41
Thermal analysis	S45
X-ray crystallography	S49
References	S50

## Experimental Section

### General

$^1\text{H}$ ,  $^{13}\text{C}$  and  $^{19}\text{F}$  NMR spectra were recorded on Bruker Avance 400 MHz, Varian Mercury 200, and 400 MHz, Varian Inova 500 MHz or Varian VNMRS 600 and 700 MHz spectrometers. All spectra were either referenced against the residual solvent signal or tetramethylsilane (TMS) and peak shifts are reported in ppm. For  $^{13}\text{C}$  NMR assignment the labels \* and # denote 2 and 3 overlapping signals, respectively. Electrospray ionisation (ESI) mass spectra were recorded on a Waters Ltd. TQD spectrometer. Atmospheric solids analysis probe (ASAP) mass spectra were recorded on a LCT premier XE spectrometer. Matrix-assisted laser desorption time-of-flight (MALDI-TOF) mass spectra were recorded on a Bruker Daltonik Autoflex II spectrometer running in positive ion reflectron mode. MALDI-TOF samples were prepared in  $\text{CH}_2\text{Cl}_2$  (DCM) with *trans*-2-[3-(4-*tert*-butylphenyl)-2-methyl-2-propenylidene]malononitrile (DCTB) as the matrix. Elemental analyses were obtained on an Exeter Analytical Inc. CE-440 elemental analyser. Thermal analysis was run under a helium atmosphere at a rate of  $10\text{ }^\circ\text{C min}^{-1}$  using a Perkin-Elmer Pyris 1 instrument. Reactions requiring an inert atmosphere were carried out under argon which was first passed through a phosphorus pentoxide column. Thin layer chromatography (TLC) was carried out on silica gel (Merck, silica gel 60, F254) or alumina (Merck, neutral alumina 60 type E, F254) plates and visualised using UV light (254, 315, 365 nm). Flash chromatography was carried out using either glass columns or a Biotage® Isolera One™ automated flash chromatography machine on 60 micron silica gel purchased from Fluorochem Ltd.

### Chemicals

All commercial chemicals were of  $\geq 95\%$  purity and were used as received without further purification. *N*-(2,2-Diethoxyethyl)mesitylamine (**S1**),<sup>1</sup> bis(trifluoromethyl)hydrazide (**2H13**) and *N,N'*-bis(pentafluorobenzoyl)hydrazide (**2H12**)<sup>2</sup> were prepared by literature procedures. All solvents used were of analytical reagent grade or higher. Anhydrous solvents were dried through a HPLC column on an Innovative Technology Inc. solvent purification system or purchased from Acros (dry diglyme).

### Calculations

All calculations were carried out with the Gaussian 09 package.<sup>3</sup> All optimised  $S_0$  geometries of the diiridium complexes were carried out using B3LYP<sup>4,5</sup> with the pseudopotential (LANL2DZ)<sup>6-8</sup> for iridium and 3-21G\* basis set for all other atoms.<sup>9,10</sup> All  $S_0$  geometries were true minima based on no imaginary frequencies found. Electronic structure calculations were also carried out on the optimised geometries at B3LYP/LANL2DZ:3-21G\*. The MO diagrams and orbital contributions were generated with the aid of Gabedit<sup>11</sup> and GaussSum<sup>12</sup> packages, respectively.

### X-ray Crystallography

X-ray diffraction experiments were carried out at 120 K on a Bruker 3-circle diffractometer D8 Venture with a PHOTON 100 CMOS area detector, using Mo- $K\alpha$  radiation from an Incoatec I $\mu$ S microsource with focussing mirrors and a Cryostream (Oxford Cryosystems) open-flow  $\text{N}_2$  gas cryostat. The absorption correction was carried out by numerical integration based on crystal face indexing, using SADABS program.<sup>13</sup> The structures were solved by Patterson or direct methods using SHELXS 2013/1 software<sup>14</sup> and refined in anisotropic approximation by full matrix least squares against  $F^2$  off all data, using SHELXL 2018/3 software<sup>15</sup> on OLEX2<sup>16</sup> platform. In both structures, the asymmetric unit comprises half of the complex molecule (which possesses a crystallographic inversion centre), as well as three DCM molecules (*meso*-**7**) or one methanol molecule (*meso*-**8**). Crystal data are listed in Table S5.

## Electrochemistry

Cyclic voltammetry experiments were recorded using either BAS CV50W electrochemical analyzer or a PalmSens EmStat<sup>2</sup> potentiostat with PSTrace software. A three-electrode system consisting of a Pt disk ( $\varnothing = 1.8$  mm) as the working electrode, a Pt wire as an auxiliary electrode and an Pt wire as a quasireference electrode was used. Cyclic voltammetry experiments were conducted at a scan rate of 100 mV/s. Experiments were conducted in dry, degassed DCM with *n*-Bu<sub>4</sub>NPF<sub>6</sub> (0.1 M) as the supporting electrolyte for oxidations, and in dry, degassed THF with *n*-Bu<sub>4</sub>NPF<sub>6</sub> (0.1 M) as the supporting electrolyte for reductions. All experiments were referenced internally to ferrocene. Oxidation processes are assigned as being electrochemically reversible based on the equal magnitudes of corresponding oxidation and reduction peaks.

## Photophysics

**General.** The absorption spectra were measured on either a Unicam UV2-100 spectrometer operated with the Unicam Vision software or a Thermo Scientific Evolution 220 spectrometer with the Thermo Scientific Insight software in quartz cuvettes with a path length of 20 mm. The pure solvent was used for the baseline correction. The extinction coefficients were calculated using the Beer-Lambert Law,  $A = \epsilon cl$ . They were measured using a titration method, whereby a stock solution of known concentration was incrementally added using a calibrated glass pipette to a cuvette of pure solvent. A minimum of 1 mg of sample was weighed for the stock solutions, and the measurements were carried out in triplicate to minimise weighing and dilution-errors. The photoluminescence spectra were recorded on a Horiba Jobin Yvon SPEX Fluorolog 3-22 spectrofluorometer in quartz cuvettes with a path length of 10 mm. All Ir complexes were measured in degassed DCM (repeated freeze-pump-thaw cycles using a turbomolecular pump). The quantum yields of all samples were determined by the comparative method relative to quinine sulphate in 0.5 M H<sub>2</sub>SO<sub>4</sub> ( $\Phi = 0.546^{17}$ ) following the literature procedure.<sup>18</sup> Poly(methyl methacrylate) films were prepared according to a literature procedure.<sup>2</sup> The quantum yields of complexes doped in PMMA thin films were recorded on a Horiba Jobin Yvon SPEX Fluorolog 3 using a calibrated Quanta- $\Phi$  integrating sphere and were calculated according to the literature method.<sup>19</sup> Solid state PLQY data were obtained in triplicate from three samples that were prepared in parallel: the calculated standard error values were  $\leq 10\%$ . Lifetime measurements were recorded using an N<sub>2</sub> laser (337 nm, 10  $\mu$ J, 10 Hz) as an excitation source in a custom spectrometer which produced a 1 kHz train of pulses of 20 ns duration. The luminescence was collected at 90° and focused onto the entrance slit of a monochromator (Bethan TM 300V). The emission was detected by a photon counting PMT and the arrival times of photons at the detector determined using a multichannel scaler. The data were transferred to a PC and analysed using non-linear regression. The decay data were fitted to exponential functions. Low temperature emission spectra and lifetime data were measured in a DN1704 optical cryostat (Oxford Instruments) with a ITC601 temperature controller (Oxford Instruments).

## Synthesis

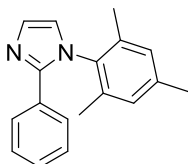
**General procedure for the synthesis of 1,2-diarylimidazoles (H9–H11).** Based on a literature procedure.<sup>20</sup>

**Step I.** Based on *ca.* 10 mmol scale of *N*-(2,2-diethoxyethyl)mesitylamine (**S1**). Triethylamine (2.00 eq.) and the benzoyl chloride derivative (5.00 eq.) were added sequentially to a solution of *N*-(2,2-diethoxyethyl)mesitylamine (**S1**) (1.00 eq.) in DCM (20 mL) under argon at 0 °C. The mixture was warmed to room temperature and stirred overnight. The solvent was then removed under reduced pressure and the residue was dissolved in acetone/ water (9:1 v/v, 20 mL). *para*-Toluenesulfonic acid (2.10 eq.) was added and the resulting mixture was heated to reflux for 2 h. The solvent was evaporated under reduced pressure and the residue was dissolved in EtOAc (80 mL). The solution was washed with sat. aq. Na<sub>2</sub>CO<sub>3</sub> (2 × 50 mL). The washings were combined and extracted with EtOAc (3 × 80 mL). All organic layers were then combined, washed with water (20 mL), dried over MgSO<sub>4</sub> and filtered. After evaporation of the solvent, the residue (**A**) was used in Step II without further purification.

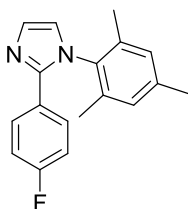
**Step II.** The product (**A**) from Step I was cautiously dissolved in acetic anhydride (15 mL). The solution was cooled to 0 °C and aq. HBF<sub>4</sub> (50%, 1.20 eq.) was added slowly. The resulting mixture was stirred overnight at room temperature. It was then added dropwise to stirred diethyl ether (100 mL) to precipitate the intermediate salt **B**. Prolonged stirring, sonication or scratching was sometimes required to induce precipitation. The solid was filtered and washed with Et<sub>2</sub>O (2 × 10 mL).

**Step III.** The product (**B**) from Step II was dissolved in MeCN (30 mL). NH<sub>4</sub>OAc (1.70 eq.) was added and the solution was stirred at room temperature for 24 h. Next, aq. HBF<sub>4</sub> (50%, 1.70 eq.) was added and the reaction mixture was heated to reflux overnight. The solvent was evaporated under reduced pressure and the residue was dissolved in EtOAc (80 mL). The solution was washed with sat. aq. Na<sub>2</sub>CO<sub>3</sub> (2 × 50 mL). The washings were combined and extracted with EtOAc (3 × 80 mL). All organic layers were then combined, washed with water (20 mL), dried over MgSO<sub>4</sub> and filtered. After evaporation of the solvent the residue was purified by flash chromatography on silica gel.

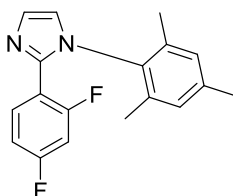
**1-(2,4,6-Trimethylphenyl)-2-phenylimidazole (H9).** The general procedure for 1,2-diarylimidazoles was followed starting from *N*-(2,2-diethoxyethyl)mesitylamine (**S1**) (6.63 g, 26.4 mmol, 1.00 eq.) and benzoyl chloride (18.6 g, 132 mmol, 5.00 eq.). The crude product was purified by flash chromatography on silica gel (eluent: gradient 1:0–6:4 *n*-hexane/ EtOAc v/v with *ca.* 0.5% NEt<sub>3</sub> as additive) to obtain 1-(2,4,6-trimethylphenyl)-2-phenylimidazole (**H9**) as an off-white powder (4.40 g, 16.7 mmol, 63%). NMR analytical data were in agreement with those previously reported.<sup>20</sup> <sup>1</sup>H NMR (400 MHz, CDCl<sub>3</sub>) δ (ppm) = 7.46 – 7.41 (m, 2H), 7.33 (d, *J* = 1.2 Hz, 1H), 7.26 – 7.20 (m, 3H), 6.99 – 6.96 (m, 2H), 6.91 (d, *J* = 1.2 Hz, 1H), 2.37 (s, 3H), 1.94 (s, 6H).



**1-(2,4,6-Trimethylphenyl)-2-(4-fluorophenyl)imidazole (H10).** The general procedure for 1,2-diarylimidazoles was followed starting from *N*-(2,2-diethoxyethyl)mesitylamine (**S1**) (3.17 g, 12.6 mmol, 1.00 eq.) and 4-fluorobenzoyl chloride (10.0 g, 63.0 mmol, 5.00 eq.). The crude product was purified by flash chromatography on silica gel (eluent: gradient 1:0–6:4 *n*-hexane/ EtOAc v/v with *ca.* 0.5% NEt<sub>3</sub> as additive) to obtain 1-(2,4,6-trimethylphenyl)-2-(4-fluorophenyl)imidazole (**H10**) as an off-white powder (2.12 g, 7.56 mmol, 60%). M.pt. 107–109 °C; <sup>1</sup>H NMR (400 MHz, CDCl<sub>3</sub>) δ (ppm) = 7.43 – 7.37 (m, 2H), 7.31 (d, *J* = 1.3 Hz, 1H), 6.98 (s, 2H), 6.96 – 6.88 (m, 3H), 2.37 (s, 3H), 1.93 (s, 6H); <sup>13</sup>C NMR (101 MHz, CDCl<sub>3</sub>) δ (ppm) = 162.6 (d, *J* = 248.4 Hz), 145.5, 139.0, 135.2, 134.4, 129.4, 129.3, 128.6 (d, *J* = 8.2 Hz), 127.0 (d, *J* = 3.4 Hz), 121.9, 115.4 (d, *J* = 21.6 Hz), 21.1, 17.6; <sup>19</sup>F{<sup>1</sup>H} NMR (376 MHz, CDCl<sub>3</sub>) δ (ppm) = -113.1 (s, 1F); HRMS (ESI): *m/z* 281.1458 [MH<sup>+</sup>]. Calcd. for C<sub>18</sub>H<sub>18</sub>FN<sub>2</sub><sup>+</sup>: 281.1454.

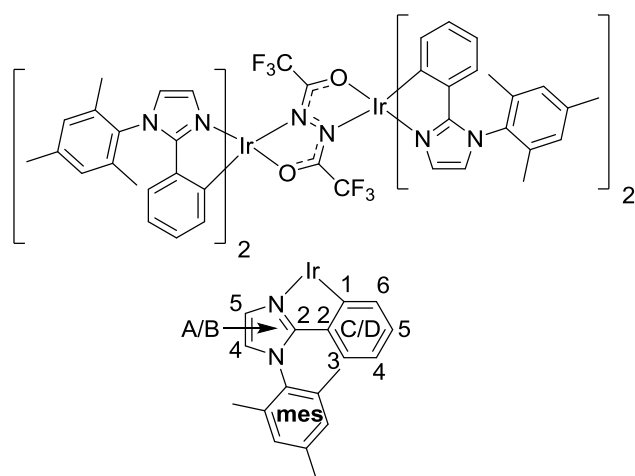


**1-(2,4,6-Trimethylphenyl)-2-(2,4-difluorophenyl)imidazole (H11).** A modification of the general procedure for 1,2-diarylimidazoles was followed starting from *N*-(2,2-diethoxyethyl)mesitylamine (**S1**)



(3.33 g, 13.2 mmol, 1.00 eq.) and 2,4-difluorobenzoyl chloride (9.30 g, 66.0 mmol, 5.00 eq.) where aq. PF<sub>6</sub> (65%, 1.20 eq.) was used instead of aq. HBF<sub>4</sub> in step II. The crude product was purified by flash chromatography on silica gel (eluent: gradient 1:0–4:6 *n*-hexane/ EtOAc v/v with *ca.* 0.5% NEt<sub>3</sub> as additive) to obtain 1-(2,4,6-trimethylphenyl)-2-(2,4-difluorophenyl)imidazole (**H11**) as an off-white powder (2.22 g, 7.39 mmol, 56%). M.pt. 80.5–82 °C; <sup>1</sup>H NMR (400 MHz, CDCl<sub>3</sub>) δ (ppm) = 7.37 (d, *J* = 1.3 Hz, 1H), 7.32 (td, *J* = 8.5, 6.4 Hz, 1H), 7.00 (d, *J* = 1.3 Hz, 1H), 6.89 (s, 2H), 6.82 (dddd, *J* = 8.7, 7.8, 2.5, 0.7 Hz, 1H), 6.74 (ddd, *J* = 10.2, 8.9, 2.5 Hz, 1H), 2.31 (s, 3H), 1.96 – 1.93 (m, 6H); <sup>13</sup>C NMR (101 MHz, CDCl<sub>3</sub>) δ (ppm) = 163.1 (dd, *J* = 251.7, 12.0 Hz), 160.3 (dd, *J* = 254.4, 12.8 Hz), 142.2 (d, *J* = 2.5 Hz), 138.6, 135.1, 133.4, 132.4 (dd, *J* = 9.7, 4.1 Hz), 129.8, 129.1, 122.1, 115.6 (dd, *J* = 14.4, 3.9 Hz), 111.4 (dd, *J* = 21.3, 3.9 Hz), 104.4 (t, *J* = 25.7 Hz), 21.0, 17.6; <sup>19</sup>F{<sup>1</sup>H} NMR (376 MHz, CDCl<sub>3</sub>) δ (ppm) = -108.2 (dd, *J* = 8.8, 0.9 Hz, 1F), -108.4 (dd, *J* = 8.9, 1.1 Hz, 1F); HRMS (ESI): *m/z* 299.1363 [MH<sup>+</sup>]. Calcd. for C<sub>18</sub>H<sub>17</sub>F<sub>2</sub>N<sub>2</sub><sup>+</sup>: 299.1360.

**Complex 5.** IrCl<sub>3</sub>·3H<sub>2</sub>O (250 mg, 0.71 mmol, 1.00 eq.) and 1-(2,4,6-trimethylphenyl)-2-phenylimidazole (**H9**)



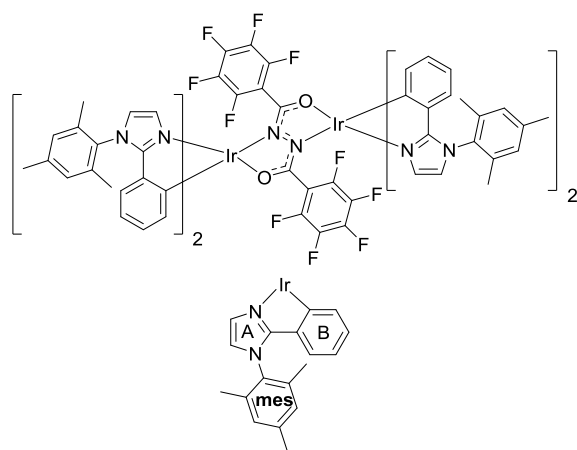
(390 mg, 1.49 mmol, 2.10 eq.) were added to 2-ethoxyethanol (10 mL) and the mixture was heated to reflux under an argon atmosphere for 24 h to form the dichloro-bridged diiridium intermediate *in situ*. The reaction mixture was then cooled to room temperature before addition of *N,N'*-bis(trifluoromethyl)hydrazide (**2H13**) (79 mg, 0.35 mmol, 0.50 eq.) and K<sub>2</sub>CO<sub>3</sub> (147 mg, 1.06 mmol, 1.49 eq.). The mixture was then heated at reflux for a further 24 h before being cooled to room temperature. The solvent was evaporated, and the residue was purified by flash chromatography on

silica gel (eluent: gradient 1:1–0:1 *n*-hexane/ DCM sat. K<sub>2</sub>CO<sub>3</sub>). After removing the solvent under reduced pressure, the residue was dissolved in a minimal amount of DCM (*ca.* 10 mL). Addition of hexane (*ca.* 20 mL) followed by reducing the volume of the mixture to 20 mL afforded complex **5** (400 mg, 0.24 mmol, 68%) as a light yellow precipitate which was isolated via filtration and washed with pentane. It was isolated as a single diastereomer. <sup>1</sup>H NMR (700 MHz, CD<sub>2</sub>Cl<sub>2</sub>, TMS) δ (ppm) = 7.28 (d, *J* = 1.5 Hz, 2H<sub>A5</sub>), 7.22 (d, *J* = 1.5 Hz, 2H<sub>B5</sub>), 7.11 – 7.07 (m, 10H<sub>A4, mesAr</sub>), 6.89 (d, *J* = 1.5 Hz, 2H<sub>B4</sub>), 6.61 (td, *J* = 7.5, 1.4 Hz, 2H<sub>C4</sub>), 6.54 (ddd, *J* = 8.1, 7.2, 1.4 Hz, 2H<sub>D4</sub>), 6.49 (td, *J* = 7.5, 1.2 Hz, 2H<sub>C5</sub>), 6.43 – 6.41 (m, 4H<sub>D3, D5</sub>), 6.25 (dd, *J* = 7.5, 1.2 Hz, 2H<sub>C3</sub>), 6.14 – 6.12 (m, 4H<sub>C6, D6</sub>), 2.41 (s, 6H<sub>mesMe</sub>), 2.41 (s, 6H<sub>mesMe</sub>), 2.13 (s, 6H<sub>mesMe</sub>), 2.08 (s, 6H<sub>mesMe</sub>), 1.96 (s, 6H<sub>mesMe</sub>), 1.95 (s, 6H<sub>mesMe</sub>); <sup>19</sup>F NMR (376 MHz, CD<sub>2</sub>Cl<sub>2</sub>) δ (ppm) = -66.4 (s, 3F); <sup>13</sup>C NMR (176 MHz, CD<sub>2</sub>Cl<sub>2</sub>, TMS) δ (ppm) = 157.9 (C<sub>A2</sub>), 157.1 (B<sub>B2</sub>), 146.5 (C<sub>D2</sub>), 144.3 (C<sub>C2</sub>), 140.0\* (C<sub>mesAr</sub>), 135.8–135.7 (C<sub>4 × mesAr</sub>), 135.7 (C<sub>C1</sub>), 135.2 (C<sub>D1</sub>), 133.8 (C<sub>D3</sub>), 133.0 (C<sub>mesAr</sub>), 132.8 (C<sub>mesAr</sub>), 132.2 (C<sub>C3</sub>), 129.4–129.3 (C<sub>4 × mesAr</sub>), 127.7 (C<sub>C4</sub>), 126.9\* (C<sub>B5, D4</sub>), 125.1 (C<sub>A5</sub>), 121.0 (C<sub>C6 or D6</sub>), 120.7 (C<sub>C5</sub>), 120.6 (C<sub>C6 or D6</sub>), 119.8 (C<sub>A4, B4</sub>), 118.9 (C<sub>D5</sub>), 20.9\* (C<sub>mesMe</sub>), 17.5\* (C<sub>mesMe</sub>), 17.0\* (C<sub>mesMe</sub>); MS (MALDI–TOF): *m/z* 1652.3 [M<sup>+</sup>]. Calcd. for C<sub>76</sub>H<sub>68</sub>F<sub>6</sub>Ir<sub>2</sub>N<sub>10</sub>O<sub>2</sub><sup>+</sup>: 1652.5; Anal. Calcd. for C<sub>76</sub>H<sub>68</sub>F<sub>6</sub>Ir<sub>2</sub>N<sub>10</sub>O<sub>2</sub>: C, 55.26; H, 4.15; N, 8.48, Calcd. for C<sub>76</sub>H<sub>68</sub>F<sub>6</sub>Ir<sub>2</sub>N<sub>10</sub>O<sub>2</sub>·0.5CH<sub>2</sub>Cl<sub>2</sub>: C, 54.23; H, 4.10; N, 8.27. Found: C, 54.40; H, 4.04; N, 8.34. Due to low solubility in organic solvents and coupling to <sup>19</sup>F nuclei, the quaternary bridge <sup>13</sup>C NMR signals were not observed. All signals that could be clearly identified in the <sup>13</sup>C, <sup>1</sup>H–<sup>13</sup>C HSQC and <sup>1</sup>H–<sup>13</sup>C HMBC NMR spectra are reported. Some of the aromatic mesityl <sup>13</sup>C environments are reported as a range due to the large number of overlapping signals.

**General procedure for the synthesis of the diarylhydrazide-bridged complexes (6–8).** IrCl<sub>3</sub>·3H<sub>2</sub>O (250 mg, 0.71 mmol, 1.00 eq.) and the 1,2-diarylimidazole cyclometallating ligand (1.49 mmol, 2.10 eq.) were added to 2-ethoxyethanol (10 mL) and the mixture was heated to reflux under an argon atmosphere for 24 h to form the

dichloro-bridged diiridium intermediate *in situ*. The reaction mixture was cooled to room temperature and the solvent was evaporated under reduced pressure. The residue was then dried under high vacuum. Next, *N,N'*-bis(pentafluorobenzoyl)hydrazide (2H12) (149 mg, 0.35 mmol, 0.50 eq.) and K<sub>2</sub>CO<sub>3</sub> (147 mg, 1.06 mmol, 1.49 eq.) were added and the mixture was suspended in dry diglyme (15 mL). It was then heated in a 120 °C heating mantle under argon overnight. The reaction was cooled to room temperature and the solvent was subsequently removed under reduced pressure. The residue was firstly purified by flash chromatography on silica gel (eluent: typically gradient *n*-hexane/ DCM sat. K<sub>2</sub>CO<sub>3</sub>) and then dissolved in minimal DCM (*ca.* 10 mL). Addition of hexane (*ca.* 20 mL) followed by reducing the volume of the mixture to 20 mL afforded the complexes as coloured precipitates which were isolated via filtration and washed with pentane.

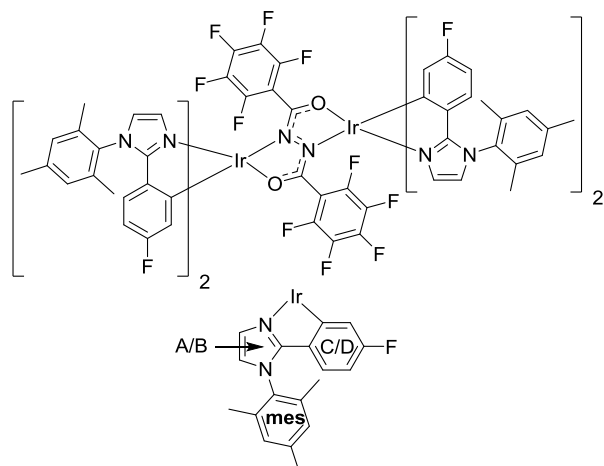
**Complex 6.** Prepared according to the general procedure, complex **6** was obtained as a light yellow powder (460



mg, 0.25 mmol, 70%). The flash chromatography eluent was DCM sat. K<sub>2</sub>CO<sub>3</sub>. **6** was obtained as a diastereomeric mixture in a *ca.* 1:1 ratio. This complicates NMR assignment of the individual diastereomers making them very difficult to distinguish and so the overlapping spectra of the mixture are reported. <sup>1</sup>H and <sup>13</sup>C Signals are assigned based on whether they represent imidazole (A), phenyl (B) or mesityl (mes) environments. Coupling constants in <sup>1</sup>H NMR are ± 0.5 Hz. <sup>1</sup>H NMR (700 MHz, CD<sub>2</sub>Cl<sub>2</sub>, TMS) δ (ppm) = 7.64 – 7.62 (m, 2H<sub>A</sub>), 7.54 (d, *J* = 1.5 Hz, 2H<sub>A</sub>), 7.49 (d, *J* = 1.6 Hz, 2H<sub>A</sub>), 7.20 (d, *J* = 1.9 Hz, 2H<sub>mesAr</sub>), 7.17 (d, *J* = 1.9 Hz, 2H<sub>mesAr</sub>), 7.13 (d, *J* =

1.5 Hz, 2H<sub>A</sub>), 7.08 (dd, *J* = 9.6, 1.6 Hz, 10H<sub>2 × A, mesAr</sub>), 7.06 – 7.04 (m, 6H<sub>mesAr</sub>), 6.97 (d, *J* = 1.5 Hz, 2H<sub>A</sub>), 6.92 (d, *J* = 1.5 Hz, 2H<sub>A</sub>), 6.53 – 6.49 (m, 4H<sub>2 × B</sub>), 6.44 – 6.39 (m, 4H<sub>2 × B</sub>), 6.37 – 6.33 (m, 2H<sub>B</sub>), 6.33 – 6.28 (m, 8H<sub>4 × B</sub>), 6.18 – 6.11 (m, 10H<sub>5 × B</sub>), 6.10 (dd, *J* = 7.7, 1.3 Hz, 2H<sub>B</sub>), 6.07 (dd, *J* = 7.8, 1.3 Hz, 2H<sub>B</sub>), 2.43 – 2.42 (m, 12H<sub>mesMe</sub>), 2.40 (s, 6H<sub>mesMe</sub>), 2.40 (s, 6H<sub>mesMe</sub>), 2.37 (s, 6H<sub>mesMe</sub>), 2.27 (s, 6H<sub>mesMe</sub>), 2.08 (s, 6H<sub>mesMe</sub>), 2.06 (s, 6H<sub>mesMe</sub>), 2.01 – 2.00 (m, 18H<sub>mesMe</sub>), 1.82 (s, 6H<sub>mesMe</sub>); <sup>19</sup>F {<sup>1</sup>H} NMR (376 MHz, CD<sub>2</sub>Cl<sub>2</sub>) δ (ppm) = -140.70 (dd, *J* = 24.7, 6.5 Hz, 2F), -141.89 (dd, *J* = 24.7, 7.2 Hz, 2F), -142.95 (dd, *J* = 24.5, 7.4 Hz, 2F), -143.87 (dd, *J* = 23.8, 7.5 Hz, 2F), -158.1 – -157.9 (m, 4F), -161.53 (td, *J* = 24.1, 22.4, 7.5 Hz, 2F), -162.14 (td, *J* = 24.2, 7.5 Hz, 2F), -163.90 (td, *J* = 23.1, 7.6 Hz, 2F), -164.79 (td, *J* = 22.9, 7.2 Hz, 2F); <sup>13</sup>C NMR (176 MHz, CD<sub>2</sub>Cl<sub>2</sub>, TMS) δ (ppm) = 183.6\* (C<sub>C=O</sub>), 157.5 (C<sub>A</sub>), 157.4 (C<sub>A</sub>), 157.3 (C<sub>A</sub>), 157.0 (C<sub>A</sub>), 148.5 (C<sub>B</sub>), 148.0 (C<sub>B</sub>), 147.3 (C<sub>B</sub>), 146.9 (C<sub>B</sub>), 139.7 (C<sub>4 × mesAr</sub>), 136.1\* (C<sub>B</sub>), 135.8 (C<sub>4 × mesAr</sub>), 135.6 (C<sub>4 × mesAr</sub>), 134.8 (C<sub>B</sub>), 134.6 (C<sub>B</sub>), 132.9 (C<sub>4 × mesAr</sub>, 2 × B), 132.5 (C<sub>2 × B</sub>), 129.5\* (C<sub>mesAr</sub>), 129.4<sup>#</sup> (C<sub>mesAr</sub>), 129.3<sup>#</sup> (C<sub>mesAr</sub>), 127.5 (C<sub>2 × B</sub>), 127.2 (C<sub>B</sub>), 127.0 (C<sub>B</sub>), 126.7\* (C<sub>A</sub>), 125.5 (C<sub>A</sub>), 125.4 (C<sub>A</sub>), 120.9 (C<sub>4 × B</sub>), 120.8 (C<sub>B</sub>), 120.6\* (C<sub>B</sub>), 120.5 (C<sub>A</sub>), 120.1 (C<sub>A</sub>), 119.8 (C<sub>A</sub>), 119.5 (C<sub>A</sub>), 118.4 (C<sub>B</sub>), 20.9\* (C<sub>mesMe</sub>), 20.8\* (C<sub>mesMe</sub>), 17.9\* (C<sub>mesMe</sub>), 17.3\* (C<sub>mesMe</sub>), 16.9 (C<sub>mesMe</sub>), 16.8 (C<sub>mesMe</sub>), 16.6 (C<sub>mesMe</sub>), 16.5 (C<sub>mesMe</sub>); MS (MALDI-TOF): *m/z* 1848.4 [M<sup>+</sup>]. Calcd. for C<sub>86</sub>H<sub>68</sub>F<sub>10</sub>Ir<sub>2</sub>N<sub>10</sub>O<sub>2</sub><sup>+</sup>: 1848.5; Anal. Calcd. for C<sub>86</sub>H<sub>68</sub>F<sub>10</sub>Ir<sub>2</sub>N<sub>10</sub>O<sub>2</sub>: C, 55.90; H, 3.71; N, 7.58, Calcd. for C<sub>86</sub>H<sub>68</sub>F<sub>10</sub>Ir<sub>2</sub>N<sub>10</sub>O<sub>2</sub>·0.3CH<sub>2</sub>Cl<sub>2</sub>: C, 55.33; H, 3.69; N, 7.48. Found: C, 55.32; H, 3.66; N, 7.46. Due to poor solubility in organic solvents and extensive coupling to <sup>19</sup>F nuclei, the <sup>13</sup>C environments corresponding to the pentafluorophenyl groups were not observed. All signals that could be clearly identified in the <sup>13</sup>C, <sup>1</sup>H-<sup>13</sup>C HSQC and <sup>1</sup>H-<sup>13</sup>C HMBC NMR spectra are reported.

**Complex 7.** Prepared according to the general procedure, complex **7** was obtained as a light yellow powder (420



mg, 0.22 mmol, 62%). The flash chromatography eluent was DCM sat.  $K_2CO_3$ . **7** was obtained as a diastereomeric mixture in a *ca.* 1:0.6 ratio. MS (MALDI-TOF):  $m/z$  1920.3 [ $M^+$ ]. Calcd. for  $C_{86}H_{64}F_{14}Ir_2N_{10}O_2^+$ : 1920.4; Anal. Calcd. for  $C_{86}H_{64}F_{14}Ir_2N_{10}O_2$ : C, 53.80; H, 3.36; N, 7.30, Calcd. for  $C_{86}H_{64}F_{14}Ir_2N_{10}O_2 \cdot 0.3CH_2Cl_2$ : C, 53.28; H, 3.35; N, 7.20. Found: C, 53.22; H, 3.27; N, 7.20.

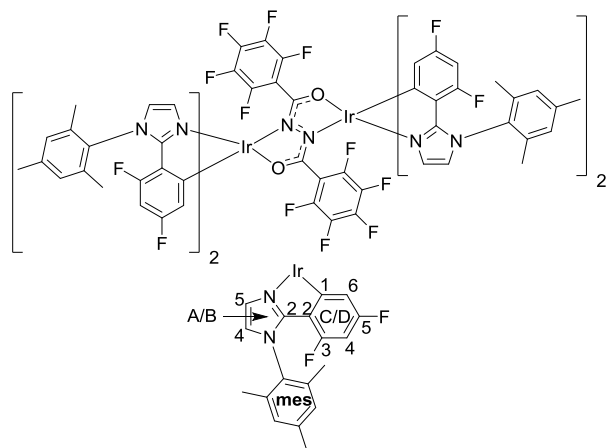
*Major diastereomer:*  $^1H$  NMR (700 MHz,  $CD_2Cl_2$ , TMS)  $\delta$  (ppm) = 7.51 (d,  $J = 1.5$  Hz,  $2H_A$ ), 7.43 (s,  $2H_B$ ), 7.18 (s,  $2H_{mesAr}$ ), 7.16 (d,  $J = 1.5$  Hz,  $2H_A$ ), 7.09

– 7.05 (m,  $6H_{3 \times mesAr}$ ), 6.93 (d,  $J = 1.5$  Hz,  $2H_B$ ), 6.18 – 6.05 (m,  $8H_{2 \times C, 2 \times D}$ ), 5.87 (dd,  $J = 10.2, 2.6$  Hz,  $2H_C$ ), 5.80 – 5.77 (m,  $2H_D$ ), 2.43 (s,  $6H_{mesMe}$ ), 2.39 (s,  $6H_{mesMe}$ ), 2.24 (s,  $6H_{mesMe}$ ), 2.07 (s,  $6H_{mesMe}$ ), 2.01 (s,  $6H_{mesMe}$ ), 1.81 (s,  $6H_{mesMe}$ );  $^{19}F$  NMR (376 MHz,  $CD_2Cl_2$ )  $\delta$  (ppm) = -113.13 (d,  $J = 1.4$  Hz, 2F), -113.35 (d,  $J = 1.4$  Hz, 2F), -141.74 (dd,  $J = 24.5, 7.6$  Hz, 2F), -142.60 (dd,  $J = 23.4, 7.6$  Hz, 2F), -157.4 – -157.5 (m, 2F), -161.29 (td,  $J = 24.5, 7.6$  Hz, 2F), -163.90 (td,  $J = 22.7, 7.9$  Hz, 2F);  $^{13}C$  NMR (176 MHz,  $CD_2Cl_2$ , TMS)  $\delta$  (ppm) = 162.6 (C!), 161.3 (C!), 156.7 ( $C_A$ ), 156.8 – 156.4 (C!), 156.2 ( $C_B$ ), 151.7 – 150.3 (C!), 139.9\* ( $C_{mesAr}$ ), 135.9 – 135.5 ( $C_{4 \times mesAr}$ ), 132.5\* ( $C_{mesAr}$ ), 132.2 (C!), 131.0 (C!), 129.7 – 129.5 ( $C_{4 \times mesAr}$ ), 126.4 ( $C_B$ ), 125.2 ( $C_A$ ), 120.8 ( $C_A$ ), 119.8 ( $C_B$ ), 118.6 ( $C_{C+D}$ ), 108.0 – 107.5 (C!), 105.6 – 105.4 (C!), 20.9\* ( $C_{mesMe}$ ), 18.0 ( $C_{mesMe}$ ), 17.3 ( $C_{mesMe}$ ), 16.5\* ( $C_{mesMe}$ ).

*Minor diastereomer:*  $^1H$  NMR (700 MHz,  $CD_2Cl_2$ , TMS)  $\delta$  (ppm) = 7.57 (d,  $J = 1.5$  Hz,  $2H_A$ ), 7.21 (s,  $2H_{mesAr}$ ), 7.09 (d,  $J = 1.5$  Hz,  $2H_A$ ), 7.09 – 7.05 (m,  $6H_{3 \times mesAr}$ ), 7.04 (d,  $J = 1.5$  Hz,  $2H_B$ ), 6.98 (d,  $J = 1.5$  Hz,  $2H_B$ ), 6.18 – 6.05 (m,  $8H_{2 \times C, 2 \times D}$ ), 5.80 – 5.77 (m,  $2H_D$ ), 5.71 (dd,  $J = 10.1, 2.6$  Hz,  $2H_C$ ), 2.43 (s,  $6H_{mesMe}$ ), 2.40 (s,  $6H_{mesMe}$ ), 2.35 (s,  $6H_{mesMe}$ ), 2.05 (s,  $6H_{mesMe}$ ), 2.01 (s,  $6H_{mesMe}$ ), 1.99 (s,  $6H_{mesMe}$ );  $^{19}F$  NMR (376 MHz,  $CD_2Cl_2$ )  $\delta$  (ppm) = -113.33 (s, 2F), -113.46 (s, 2F), -140.57 (dd,  $J = 24.2, 6.8$  Hz, 2F), -143.33 (dd,  $J = 23.0, 6.0$  Hz, 2F), -157.4 – -157.5 (m, 2F), -160.83 (td,  $J = 24.7, 8.0$  Hz, 2F), -164.37 (td,  $J = 21.4, 7.3$  Hz, 2F);  $^{13}C$  NMR (176 MHz,  $CD_2Cl_2$ , TMS)  $\delta$  (ppm) = 162.6 (C!), 161.3 (C!), 156.8 – 156.4 (C!), 156.7 ( $C_A$ ), 156.4 ( $C_B$ ), 151.7 – 150.3 (C!), 139.2\* ( $C_{mesAr}$ ), 135.9 – 135.5 ( $C_{4 \times mesAr}$ ), 132.5\* ( $C_{mesAr}$ ), 132.2 (C!), 131.0 (C!), 129.7 – 129.5 ( $C_{4 \times mesAr}$ ), 126.4 ( $C_A$ ), 125.2 ( $C_B$ ), 120.4 ( $C_A$ ), 120.1 ( $C_B$ ), 118.6 ( $C_D$ ), 118.1 ( $C_C$ ), 108.0 – 107.5 (C!), 105.6 – 105.4 (C!), 20.9\* ( $C_{mesMe}$ ), 18.0 ( $C_{mesMe}$ ), 17.3 ( $C_{mesMe}$ ), 16.8 ( $C_{mesMe}$ ), 11.9 ( $C_{mesMe}$ ).

Due to poor solubility in organic solvents and extensive coupling to  $^{19}F$  nuclei, some quaternary  $^{13}C$  environments were not observed. As many of the signals corresponding to rings C and D heavily overlap in the  $^1H$  NMR spectrum of the diastereomeric mixture, their  $^{13}C$  environments could not be unambiguously assigned to a ring or diastereomer. Such signals/ regions are labelled “!”. All signals that could be clearly identified in the  $^{13}C$ ,  $^1H$ - $^{13}C$  HSQC and  $^1H$ - $^{13}C$  HMBC NMR spectra are reported. Single crystals suitable for X-ray diffraction were grown by vapour diffusion of hexane into a DCM solution of the complex.

**Complex 8.** Prepared according to the general procedure, complex **8** was obtained as a tan powder (334 mg, 0.17 mmol, 47%). The flash chromatography eluent was gradient 9:1–4:6 *n*-hexane/ DCM sat. K<sub>2</sub>CO<sub>3</sub> v/v.



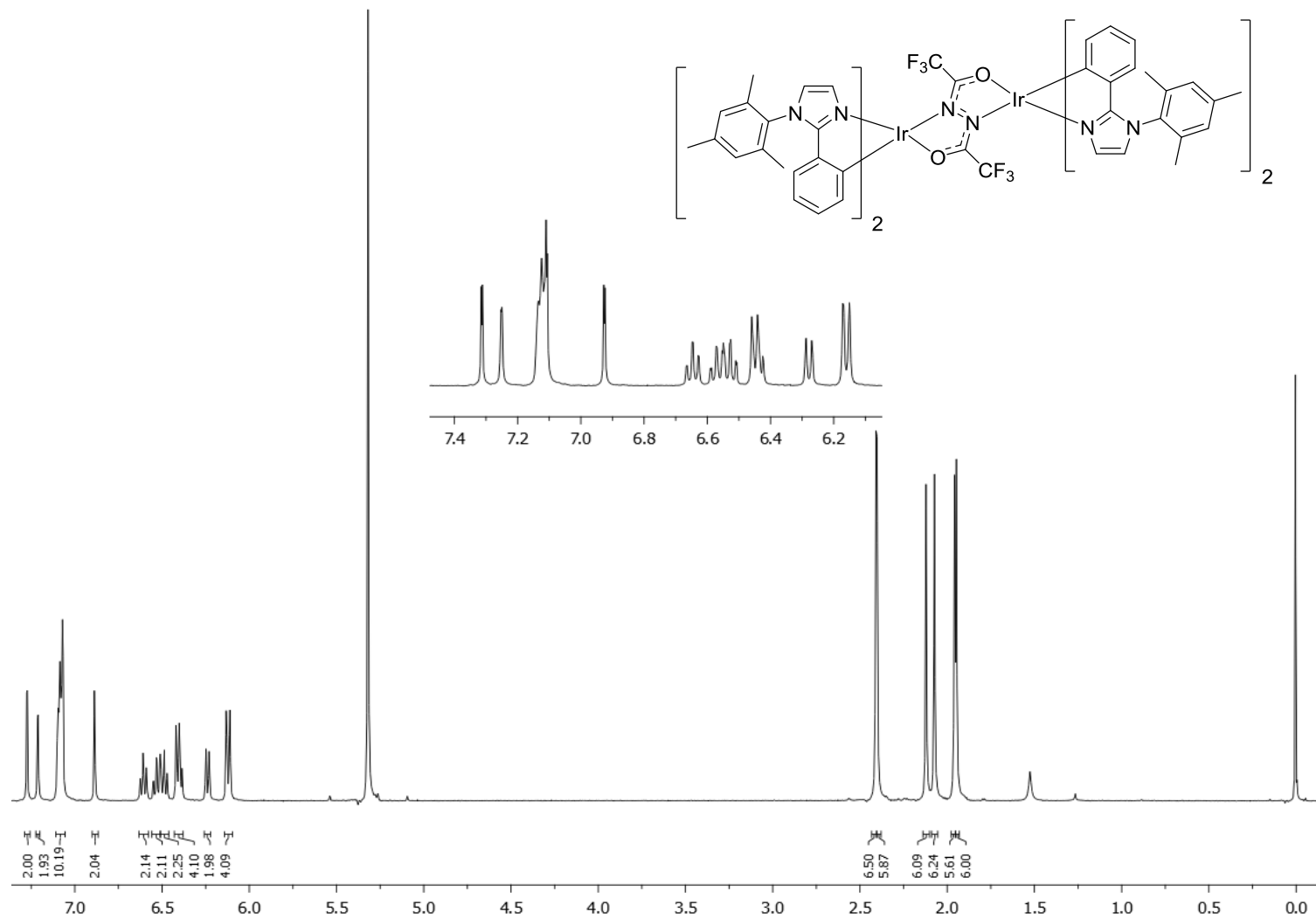
During precipitation the compound gelled, implying a propensity to interact with DCM. This is evident from the CHN result and residual DCM observed in the <sup>1</sup>H NMR spectrum of the complex after drying. **8** was obtained as a diastereomeric mixture in a *ca.* 1:0.9 ratio. MS (MALDI–TOF): *m/z* 1992.1 [M<sup>+</sup>]. Calcd. for C<sub>86</sub>H<sub>60</sub>F<sub>18</sub>Ir<sub>2</sub>N<sub>10</sub>O<sub>2</sub><sup>+</sup>: 1992.4; Anal. Calcd. for C<sub>86</sub>H<sub>60</sub>F<sub>18</sub>Ir<sub>2</sub>N<sub>10</sub>O<sub>2</sub>: C, 51.86; H, 3.04; N, 7.03, Calcd. for C<sub>86</sub>H<sub>60</sub>F<sub>18</sub>Ir<sub>2</sub>N<sub>10</sub>O<sub>2</sub>·1CH<sub>2</sub>Cl<sub>2</sub>: C, 50.31; H, 3.01; N, 6.74. Found: C, 50.31; H, 2.92; N, 6.79.

**Major diastereomer:** <sup>1</sup>H NMR (700 MHz, THF-*d*<sub>8</sub>) δ (ppm) = 7.66 (d, *J* = 1.5 Hz, 2H<sub>A5</sub>), 7.31 (d, *J* = 1.5 Hz, 2H<sub>A4</sub>), 7.25 (d, *J* = 1.6 Hz, 2H<sub>B5</sub>), 7.11 (d, *J* = 2.0 Hz, 2H<sub>mesAr</sub>), 7.09 (d, *J* = 1.6 Hz, 2H<sub>B4</sub>), 7.00 (bs, 4H<sub>mesAr</sub>), 6.99 (s, 2H<sub>mesAr</sub>), 6.01 (ddd, *J* = 11.3, 8.9, 2.4 Hz, 2H<sub>D4</sub>), 5.96 (ddd, *J* = 11.5, 9.0, 2.4 Hz, 2H<sub>C4</sub>), 5.64 (dd, *J* = 9.0, 2.4 Hz, 2H<sub>D6</sub>), 5.58 (dd, *J* = 9.1, 2.4 Hz, 2H<sub>C6</sub>), 2.39 (s, 6H<sub>mesMe</sub>), 2.37 (s, 6H<sub>mesMe</sub>), 2.34 (s, 6H<sub>mesMe</sub>), 2.04 (s, 6H<sub>mesMe</sub>), 2.02–2.00 (m, 12H<sub>mesMe</sub>); <sup>19</sup>F{<sup>1</sup>H} NMR (376 MHz, THF-*d*<sub>8</sub>) δ (ppm) = -105.78 (d, *J* = 7.9 Hz, 2F), -106.45 – -106.55 (m, 2F), -112.32 (d, *J* = 7.9 Hz, 2F), -112.70 – -112.80 (m, 2F), -141.07 (dd, *J* = 24.4, 6.4 Hz, 2F), -143.23 (dd, *J* = 24.4, 7.1 Hz, 2F), -158.18 – -158.28 (m, 2F), -162.45 (td, *J* = 24.3, 7.4 Hz, 2F), -164.82 (td, *J* = 22.0, 21.5, 7.1 Hz, 2F); <sup>13</sup>C NMR (176 MHz, THF-*d*<sub>8</sub>) δ (ppm) = 164.3 (d, *J* = 250 Hz, C<sub>D5</sub>), 164.0 (d, *J* = 250 Hz, C<sub>C5</sub>), 159.0 (d, *J* = 247 Hz, C<sub>C3</sub>), 158.2 (C<sub>A2</sub>), 158.0 (d, *J* = 264 Hz, C<sub>D3</sub>), 157.5 (C<sub>B2</sub>), 140.5\* (C<sub>mesAr</sub>), 137.7 (C<sub>mesAr</sub>), 137.6 (C<sub>mesAr</sub>), 137.5 (C<sub>mesAr</sub>), 137.0\* (C<sub>mesAr</sub>), 136.7 (C<sub>mesAr</sub>), 130.6 (C<sub>mesAr</sub>), 130.3 (C<sub>mesAr</sub>), 130.2 (C<sub>mesAr</sub>), 130.1 (C<sub>mesAr</sub>), 128.4 (C<sub>A5</sub>), 127.3 (C<sub>B4</sub>), 124.1 (C<sub>A4</sub>), 123.7 (C<sub>B5</sub>), 121.0 (C<sub>D2</sub>), 120.0 (C<sub>C2</sub>), 116.3 (d, *J* = 16.9 Hz, C<sub>D6</sub>), 116.0 (d, *J* = 16.7 Hz, C<sub>C6</sub>), 98.0 (t, *J* = 25 Hz, C<sub>D4</sub>), 96.2 (t, *J* = 25 Hz, C<sub>C4</sub>), 22.0\* (C<sub>mesMe</sub>), 19.1 (C<sub>mesMe</sub>), 18.5 (C<sub>mesMe</sub>), 18.4 (C<sub>mesMe</sub>), 18.2 (C<sub>mesMe</sub>).

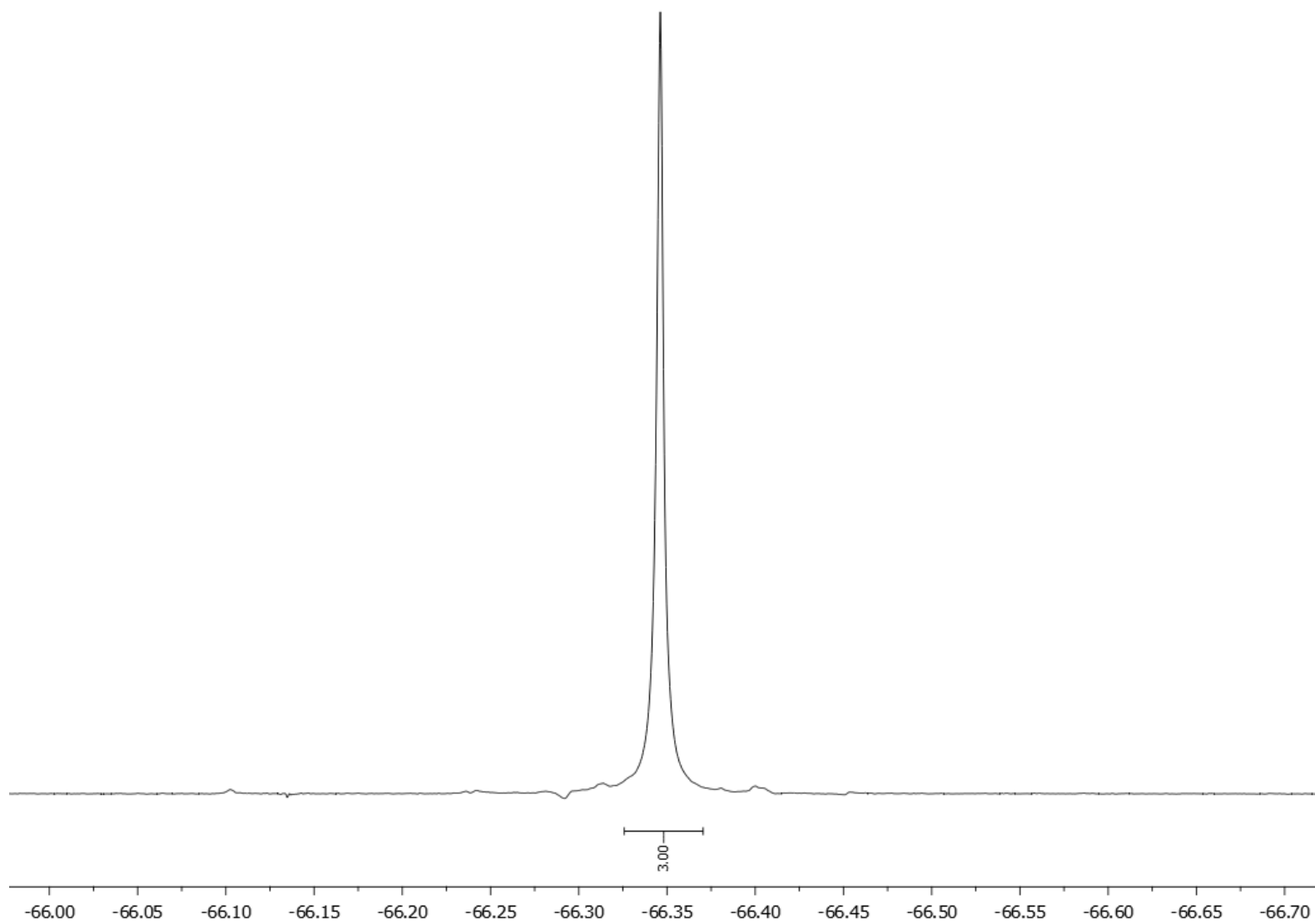
**Minor diastereomer:** <sup>1</sup>H NMR (700 MHz, THF-*d*<sub>8</sub>) δ (ppm) = 7.56 (d, *J* = 1.5 Hz, 2H<sub>A5</sub>), 7.51 (d, *J* = 1.7 Hz, 2H<sub>B5</sub>), 7.39 (d, *J* = 1.5 Hz, 2H<sub>A4</sub>), 7.17 (d, *J* = 1.7 Hz, 2H<sub>B4</sub>), 7.12 – 7.10 (m, 2H<sub>mesAr</sub>), 7.08 (s, 2H<sub>mesAr</sub>), 7.00 – 6.97 (m, 2H<sub>mesAr</sub>), 6.97 (s, 2H<sub>mesAr</sub>), 6.02 – 5.98 (m, 2H<sub>C4</sub>), 5.96 – 5.92 (m, 2H<sub>D4</sub>), 5.74 (dd, *J* = 9.2, 2.3 Hz, 2H<sub>D6</sub>), 5.61 (dd, *J* = 9.0, 2.4 Hz, 2H<sub>C6</sub>), 2.40 (s, 6H<sub>mesMe</sub>), 2.28 (s, 6H<sub>mesMe</sub>), 2.08 (s, 6H<sub>mesMe</sub>), 2.04 (s, 6H<sub>mesMe</sub>), 2.02 – 1.99 (m, 6H<sub>mesMe</sub>), 1.86 (s, 6H<sub>mesMe</sub>); <sup>19</sup>F{<sup>1</sup>H} NMR (376 MHz, THF-*d*<sub>8</sub>) δ (ppm) = -105.71 (d, *J* = 8.0 Hz, 2F), -106.45 – -106.55 (m, 2F), -111.87 (d, *J* = 8.0 Hz, 2F), -112.70 – 112.80 (m, 2F), -142.25 (dd, *J* = 24.7, 7.7 Hz, 2F), -142.54 (dd, *J* = 24.7, 7.2 Hz, 2F), -158.18 – -158.28 (m, 2F), -162.72 (td, *J* = 23.7, 7.2 Hz, 2F), -164.12 (td, *J* = 23.7, 7.7 Hz, 2F); <sup>13</sup>C NMR (176 MHz, THF-*d*<sub>8</sub>) δ (ppm) = 164.4 (d, *J* = 250 Hz, C<sub>D5</sub>), 164.1 (d, *J* = 250 Hz, C<sub>C5</sub>), 159.3 (d, *J* = 245 Hz, C<sub>C3</sub>), 158.3 (d, *J* = 260 Hz, C<sub>D3</sub>), 157.7 (C<sub>A2 + B2</sub>), 140.6\* (C<sub>mesAr</sub>), 137.9 (C<sub>mesAr</sub>), 137.6 (C<sub>mesAr</sub>), 137.5 (C<sub>mesAr</sub>), 137.0\* (C<sub>mesAr</sub>), 136.7 (C<sub>mesAr</sub>), 130.5 (C<sub>mesAr</sub>), 130.4 (C<sub>mesAr</sub>), 130.3 (C<sub>mesAr</sub>), 130.2 (C<sub>mesAr</sub>), 128.5 (C<sub>B5</sub>), 127.3 (C<sub>A5</sub>), 124.4 (C<sub>A4</sub>), 123.6 (C<sub>B4</sub>), 120.9 (C<sub>C2</sub>), 120.0 (C<sub>D2</sub>), 116.3 (d, *J* = 17 Hz, C<sub>D6</sub>), 116.0 (d, *J* = 16 Hz, C<sub>C6</sub>), 98.0 (t, *J* = 27 Hz, C<sub>C4</sub>), 96.0 (t, *J* = 26 Hz, C<sub>D4</sub>), 21.90\* (C<sub>mesMe</sub>), 19.1 (C<sub>mesMe</sub>), 18.5 (C<sub>mesMe</sub>), 18.1 (C<sub>mesMe</sub>), 17.8 (C<sub>mesMe</sub>).

Due to poor solubility in organic solvents and extensive coupling to <sup>19</sup>F nuclei, some quaternary <sup>13</sup>C environments were not observed (bridge carbons, C1 and D1). All signals that could be clearly identified in the <sup>13</sup>C, <sup>1</sup>H–<sup>13</sup>C HSQC and <sup>1</sup>H–<sup>13</sup>C HMBC NMR spectra are reported. Single crystals suitable for X-ray diffraction were grown by vapour diffusion of methanol into a THF solution of the complex.

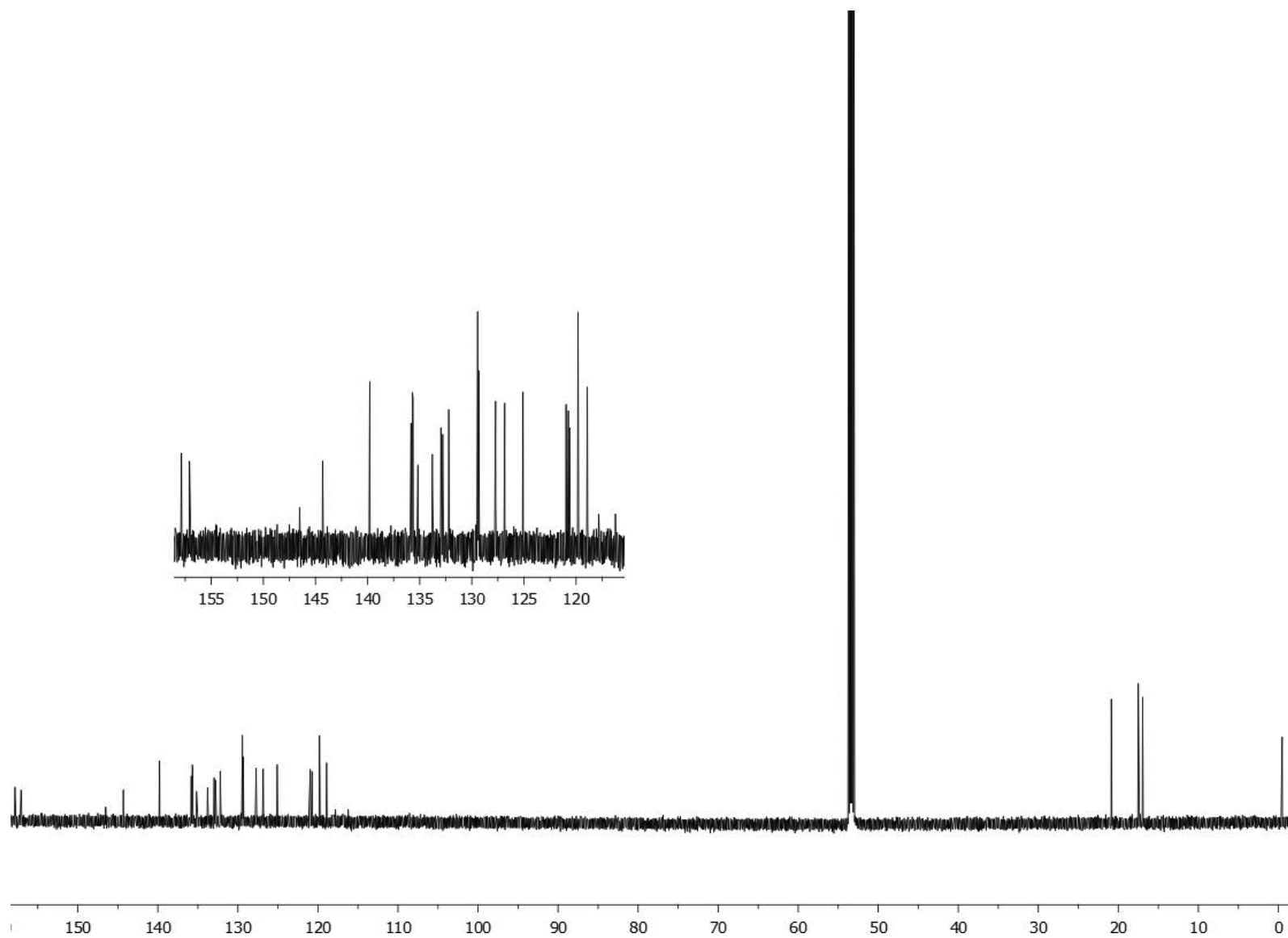
## Copies of NMR Spectra



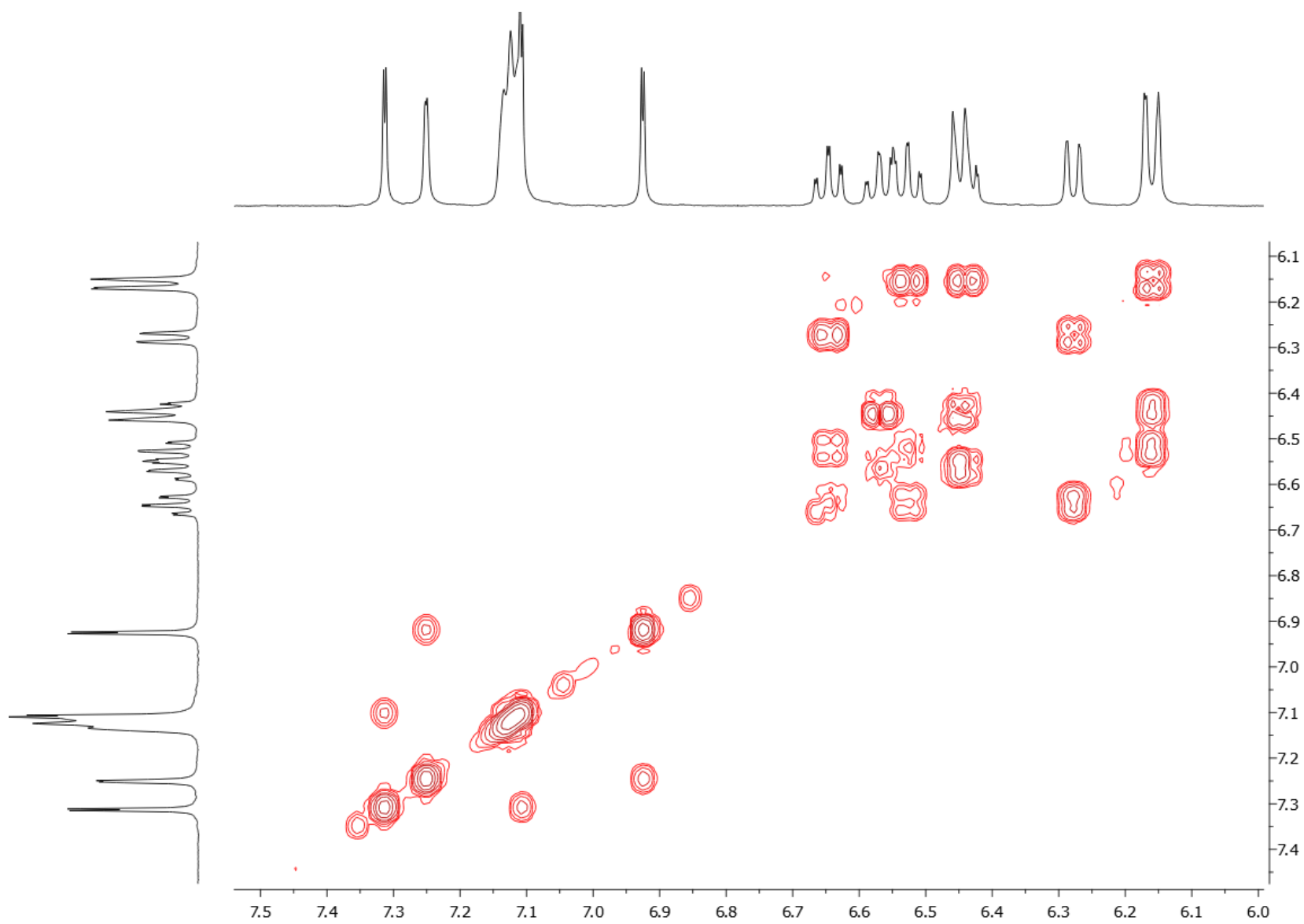
**Spectrum S1.** <sup>1</sup>H NMR spectrum (700 MHz) of **5** in CD<sub>2</sub>Cl<sub>2</sub> (TMS).



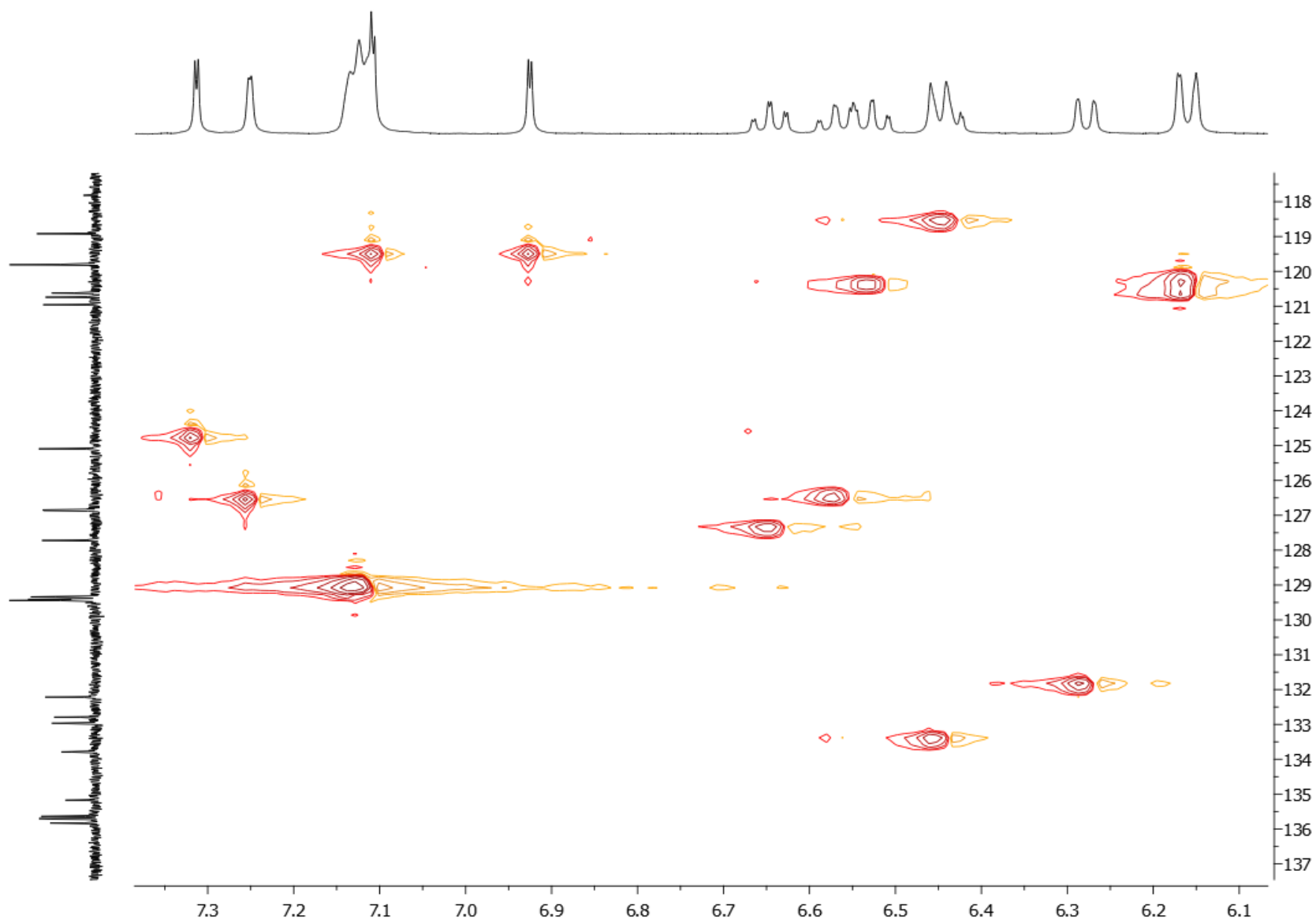
**Spectrum S2.**  $^{19}\text{F}\{^1\text{H}\}$  NMR spectrum (376 MHz) of **5** in  $\text{CD}_2\text{Cl}_2$ .



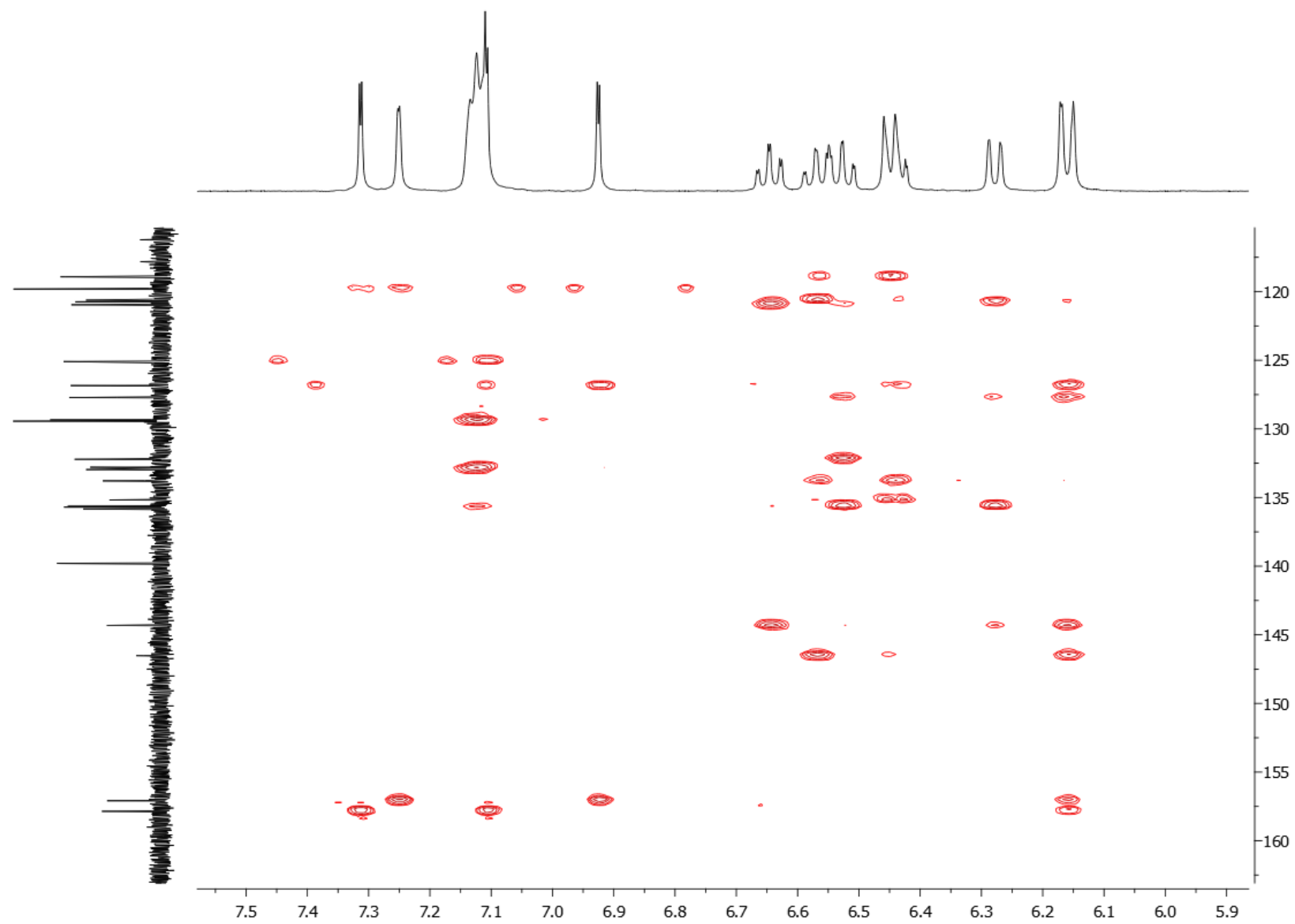
**Spectrum S3.**  $^{13}\text{C}$  NMR spectrum (151 MHz) of **5** in  $\text{CD}_2\text{Cl}_2$  (TMS).



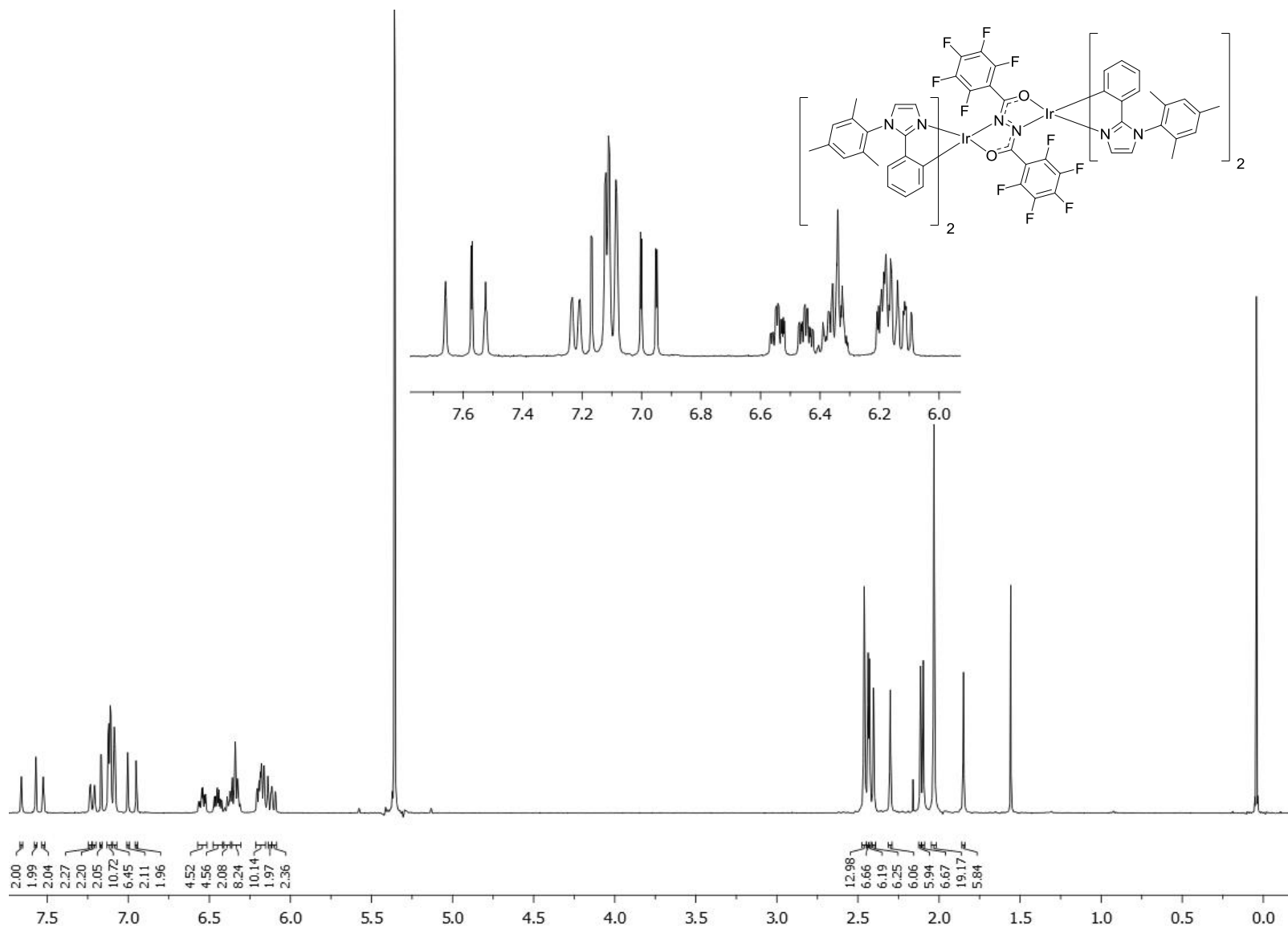
**Spectrum S4.** Expansion of the aromatic region of the  $^1\text{H}$ - $^1\text{H}$  COSY NMR spectrum of **5** in  $\text{CD}_2\text{Cl}_2$  (TMS).



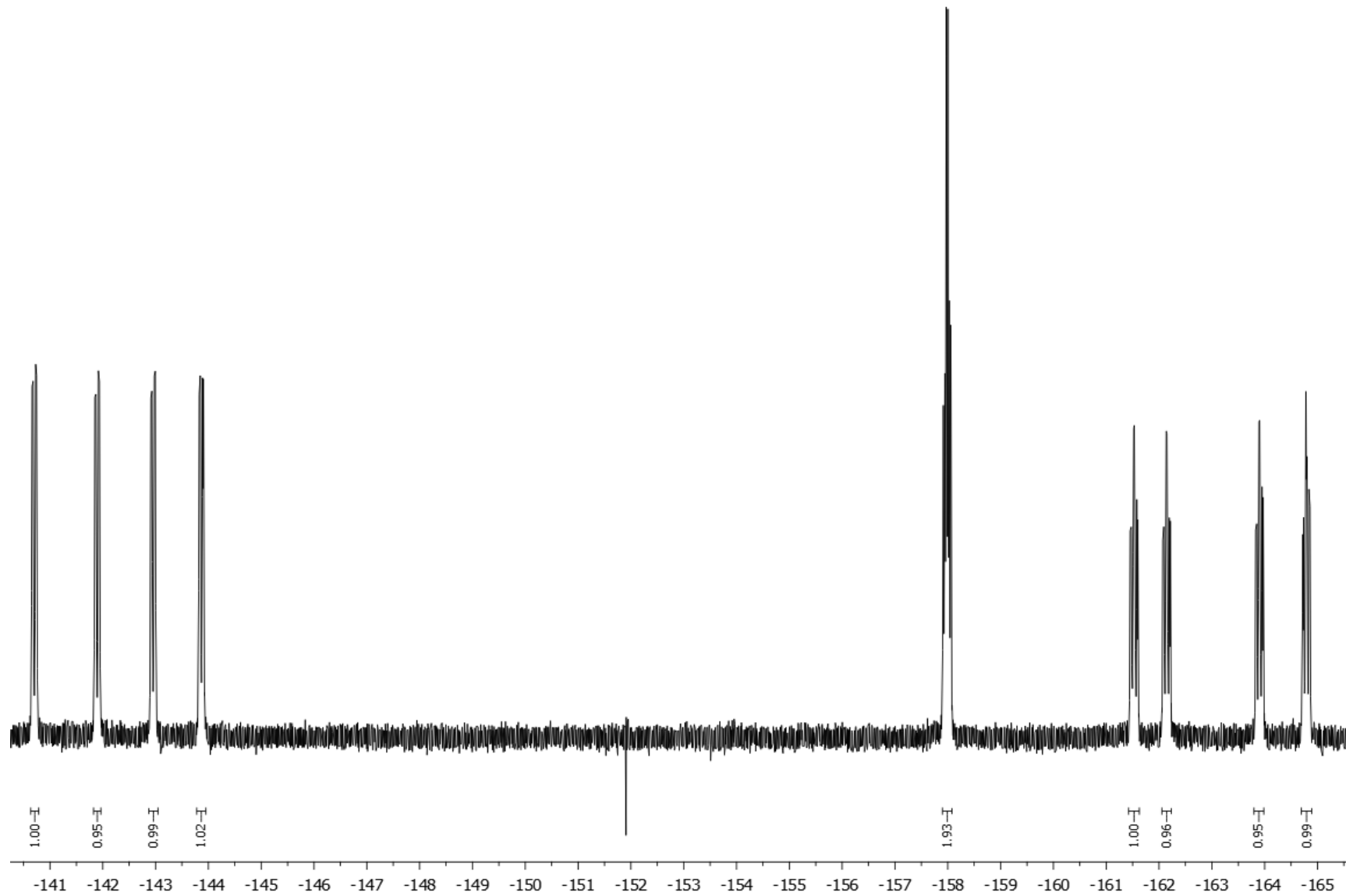
**Spectrum S5.** Expansion of the aromatic region of the  $^1\text{H}$ - $^{13}\text{C}$  HSQC NMR spectrum of **5** in  $\text{CD}_2\text{Cl}_2$  (TMS).



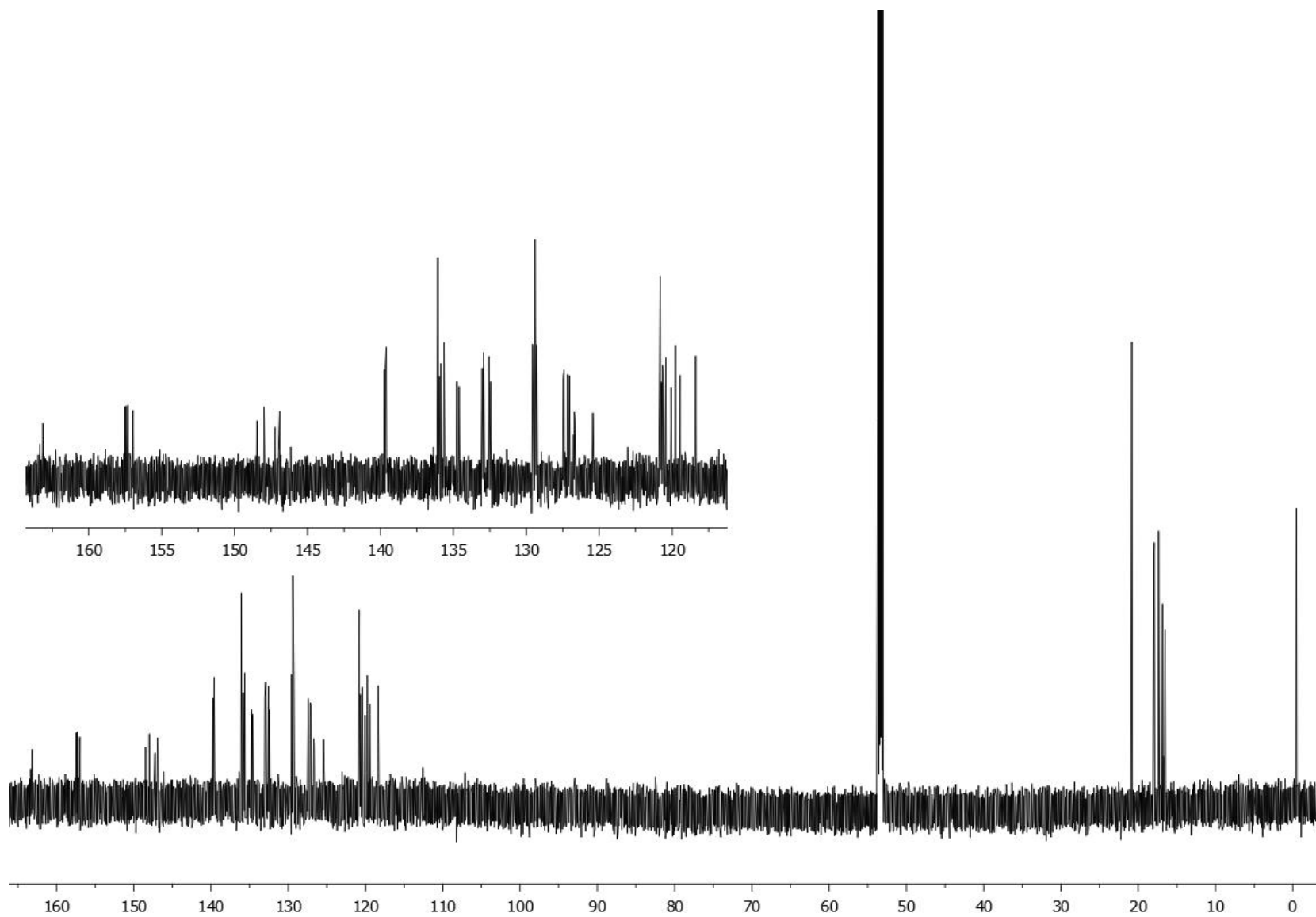
**Spectrum S6.** Expansion of the aromatic region of the  $^1\text{H}$ - $^{13}\text{C}$  HMBC NMR spectrum of **5** in  $\text{CD}_2\text{Cl}_2$  (TMS).



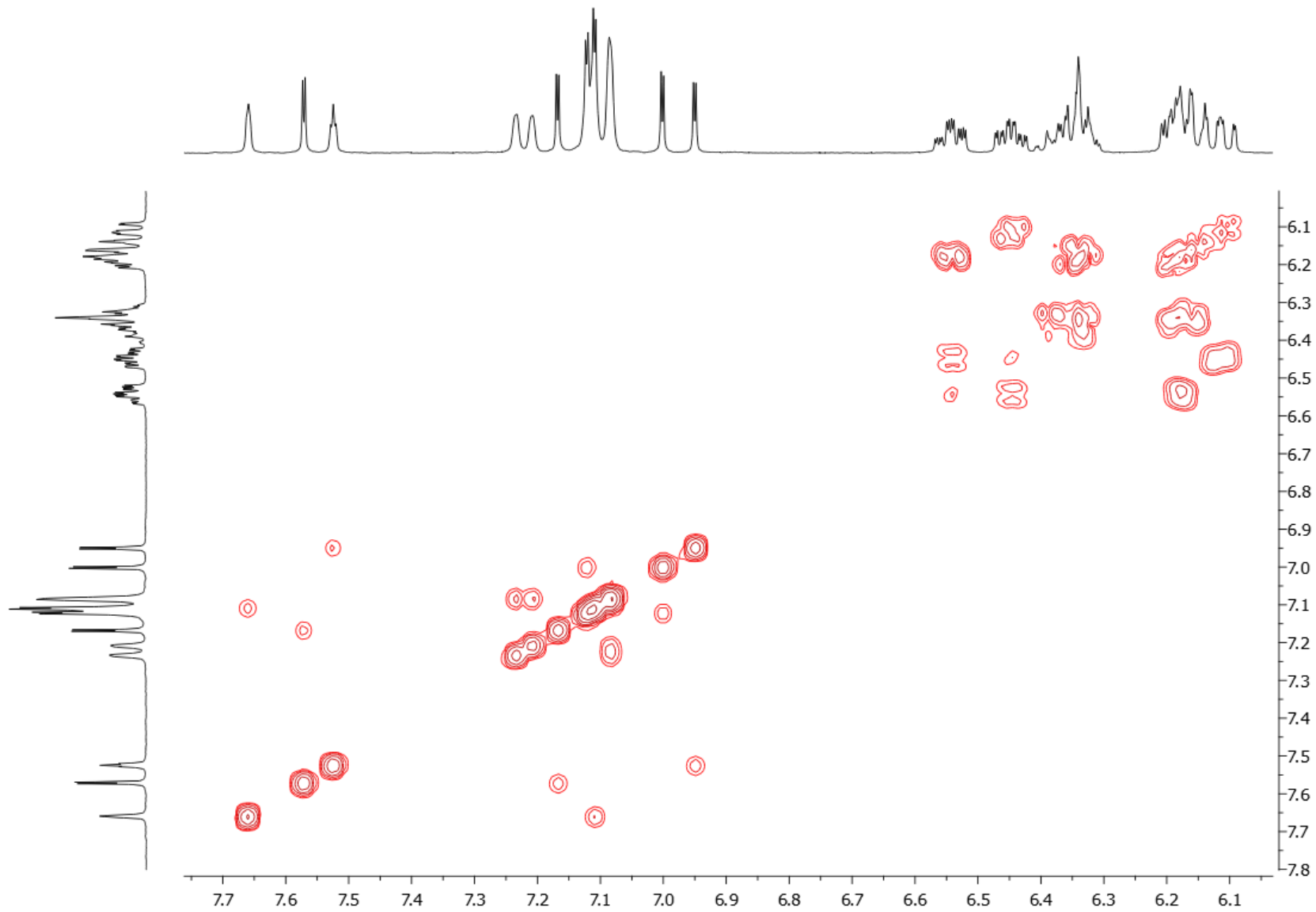
**Spectrum S7.** <sup>1</sup>H NMR spectrum (700 MHz) of **6** in CD<sub>2</sub>Cl<sub>2</sub> (TMS).



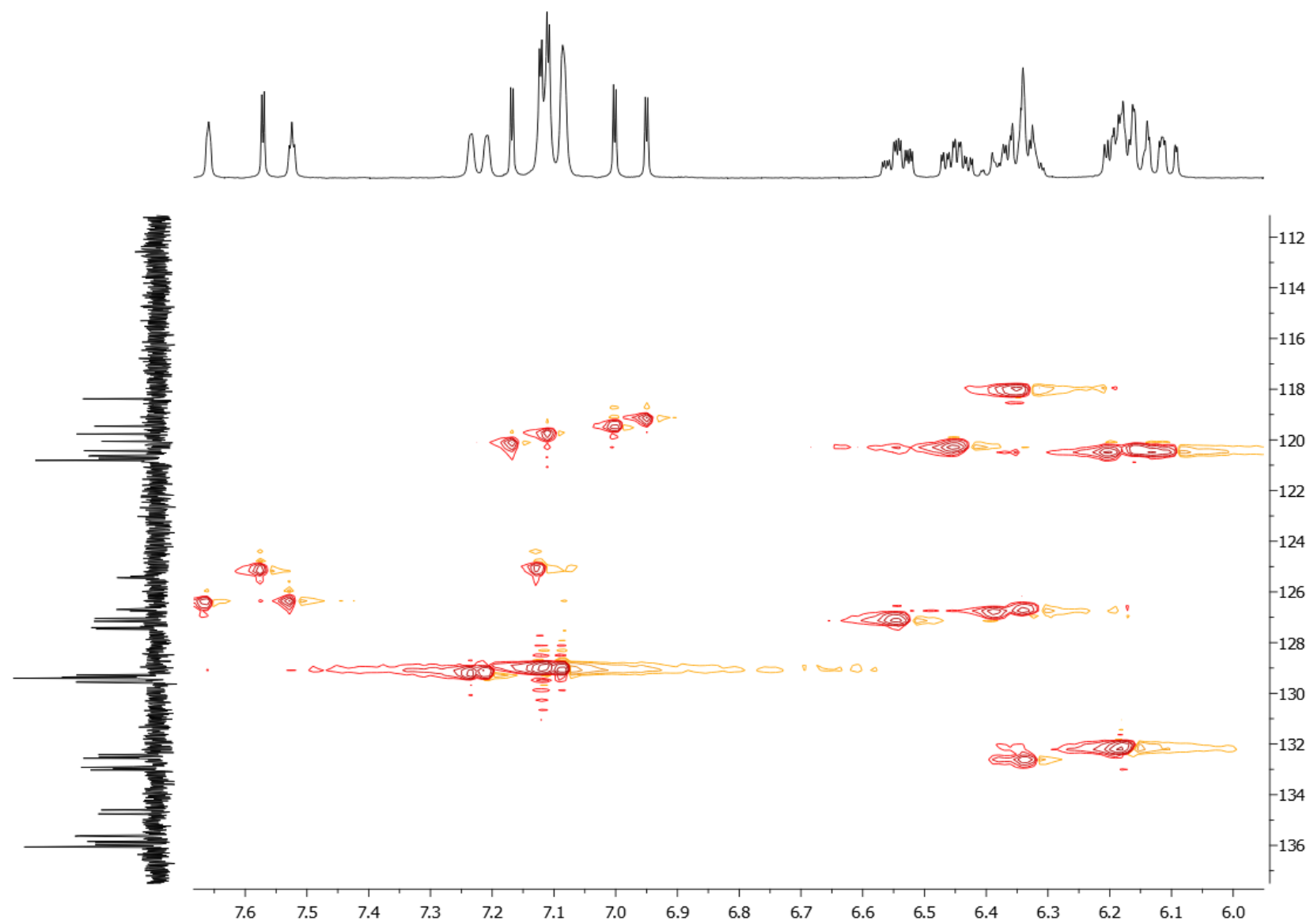
**Spectrum S8.**  $^{19}\text{F}\{^1\text{H}\}$  NMR spectrum (376 MHz) of **6** in  $\text{CD}_2\text{Cl}_2$ .



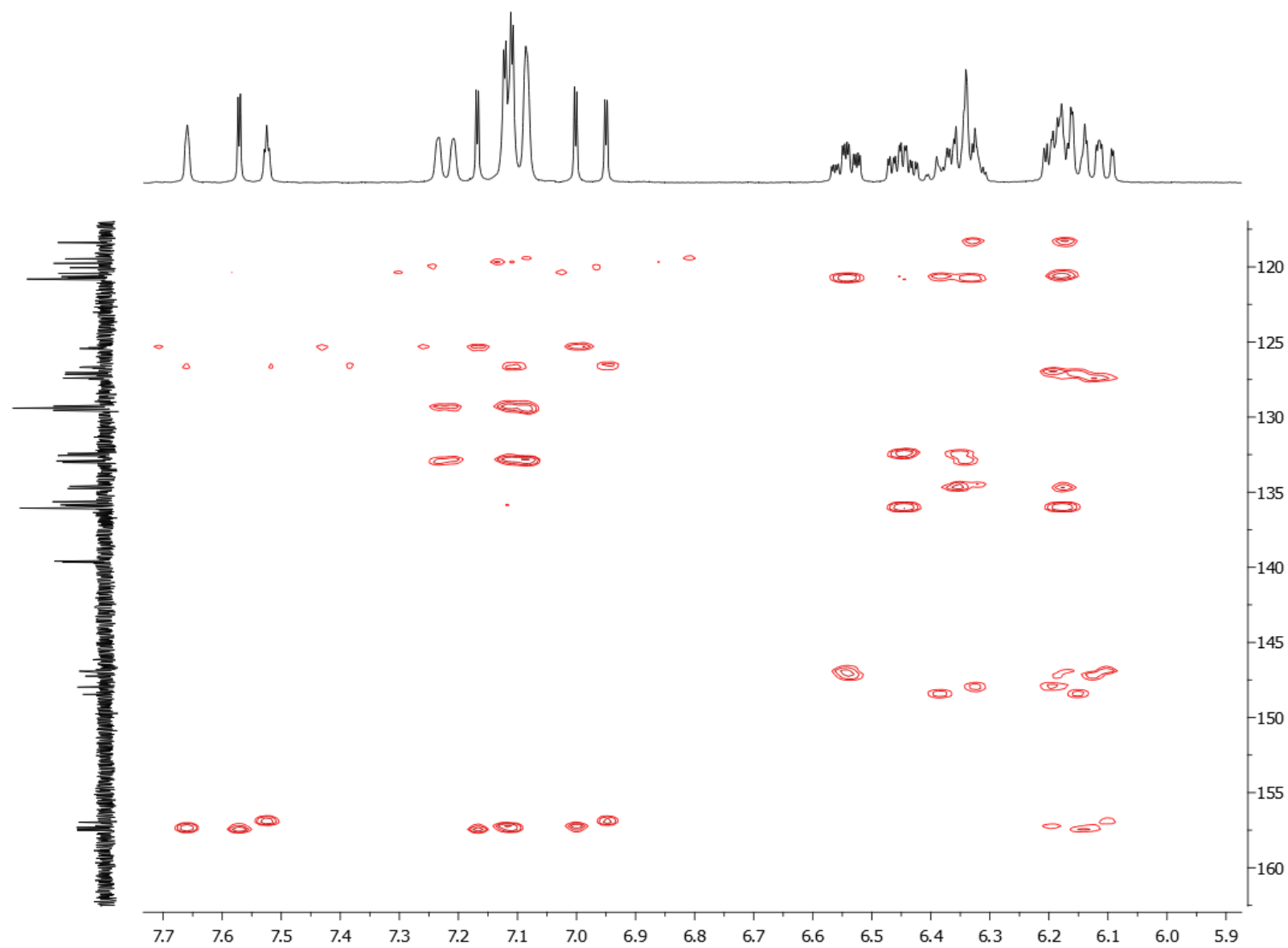
**Spectrum S9.** <sup>13</sup>C NMR spectrum (151 MHz) of **6** in CD<sub>2</sub>Cl<sub>2</sub> (TMS).



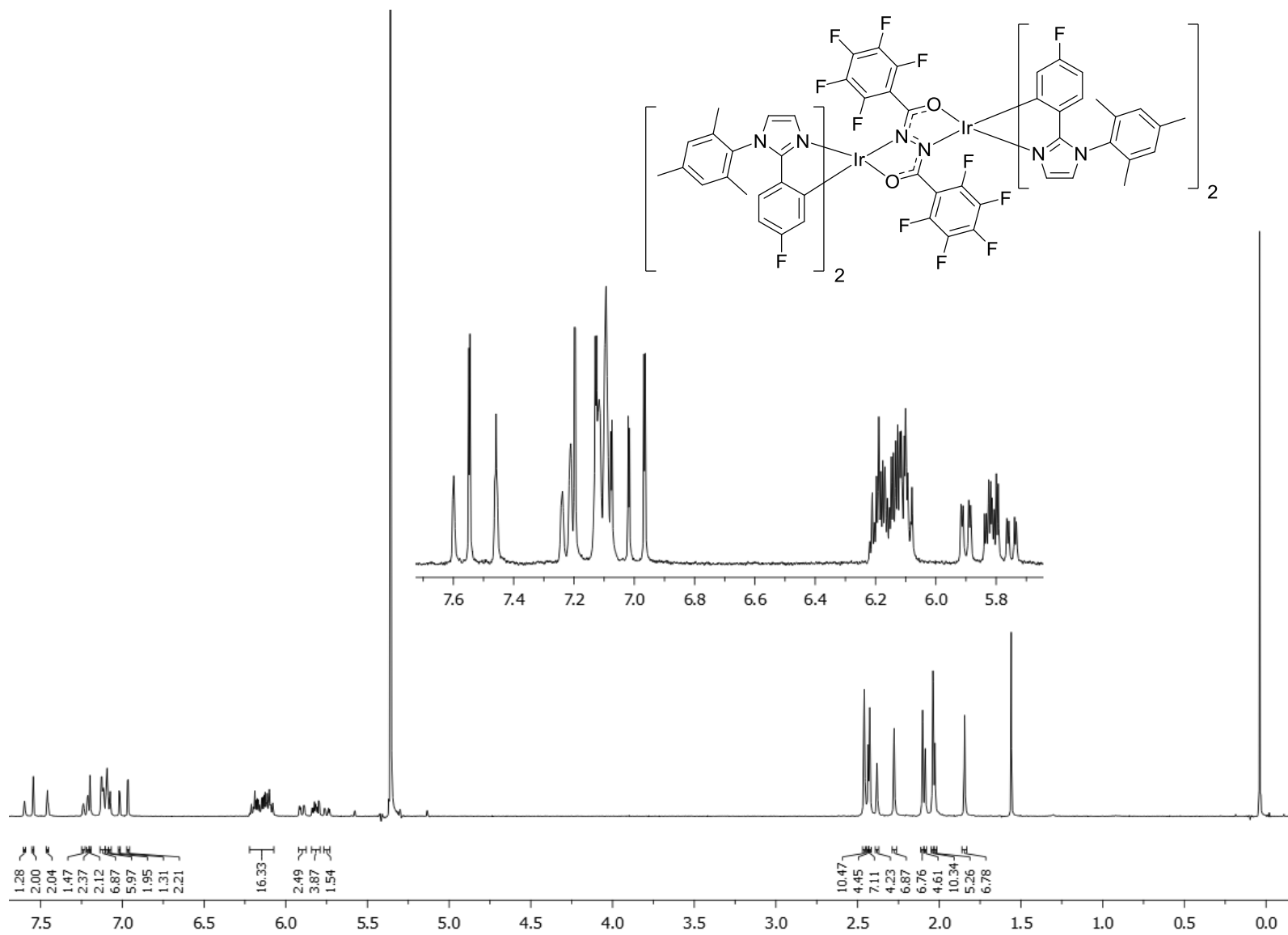
**Spectrum S10.** Expansion of the aromatic region of the  $^1\text{H}$ - $^1\text{H}$  COSY NMR spectrum of **6** in  $\text{CD}_2\text{Cl}_2$  (TMS).



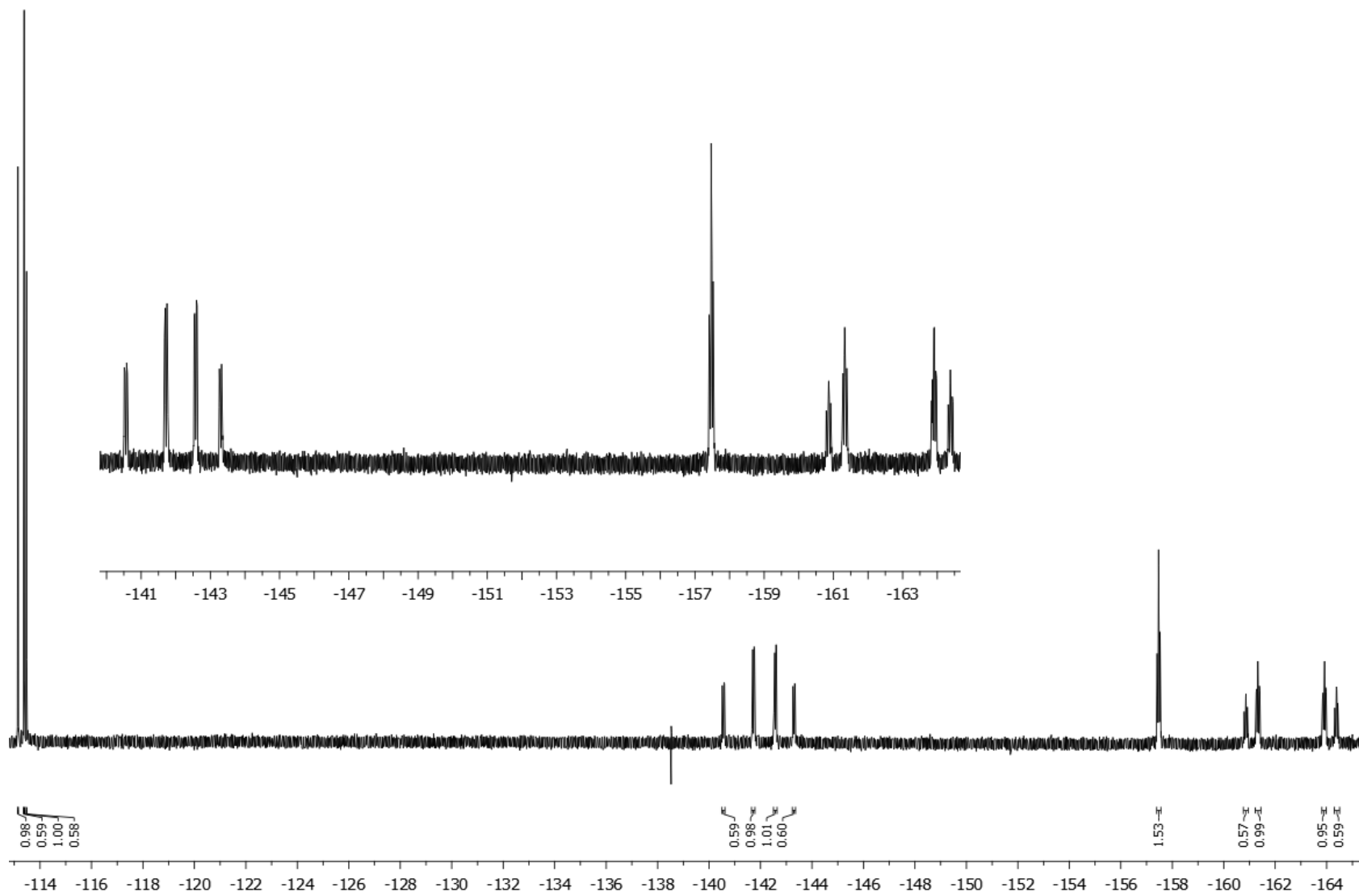
**Spectrum S11.** Expansion of the aromatic region of the  $^1\text{H}$ - $^{13}\text{C}$  HSQC NMR spectrum of **6** in  $\text{CD}_2\text{Cl}_2$  (TMS).



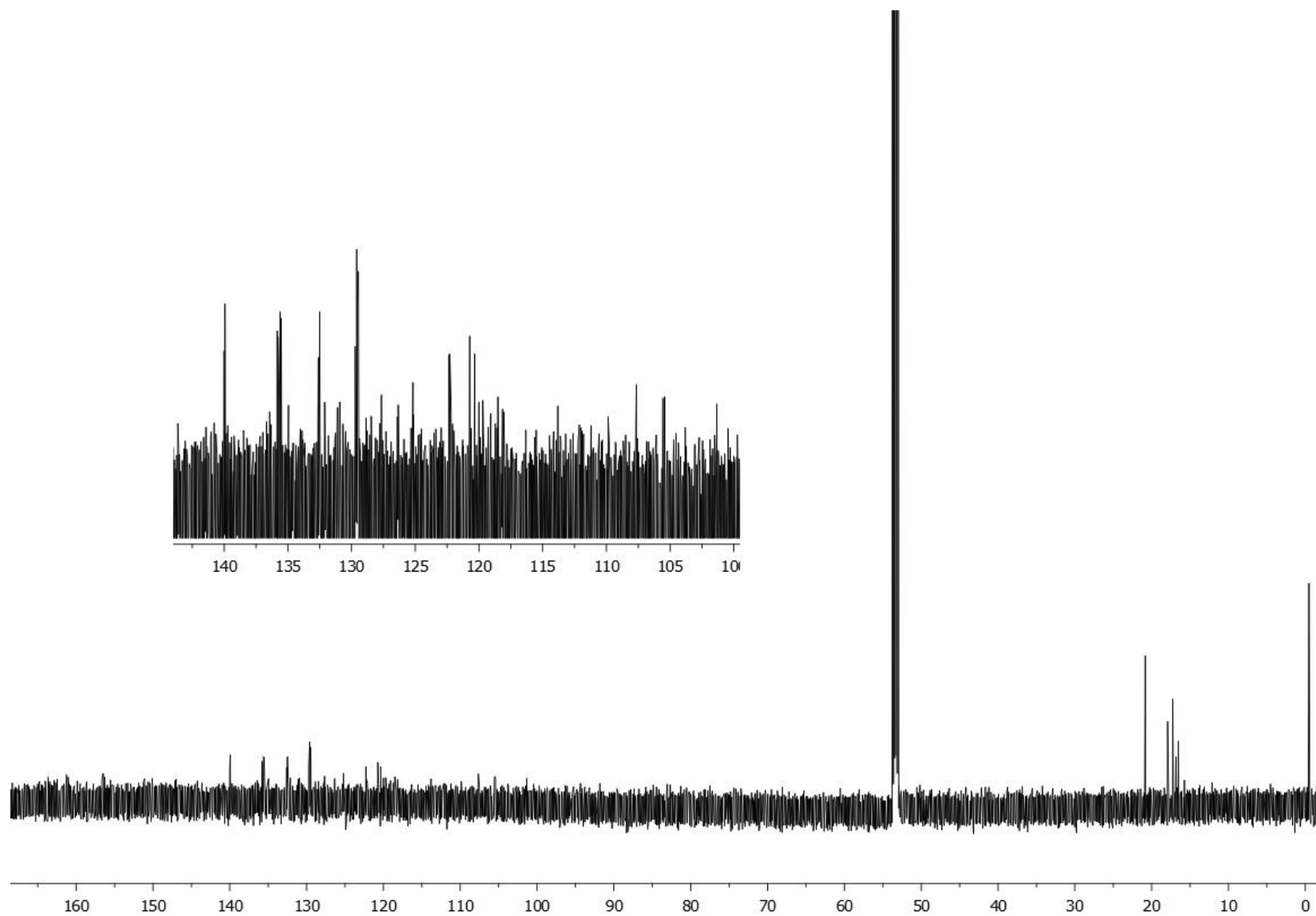
**Spectrum S12.** Expansion of the aromatic region of the  $^1\text{H}$ - $^{13}\text{C}$  HMBC NMR spectrum of **6** in  $\text{CD}_2\text{Cl}_2$  (TMS).



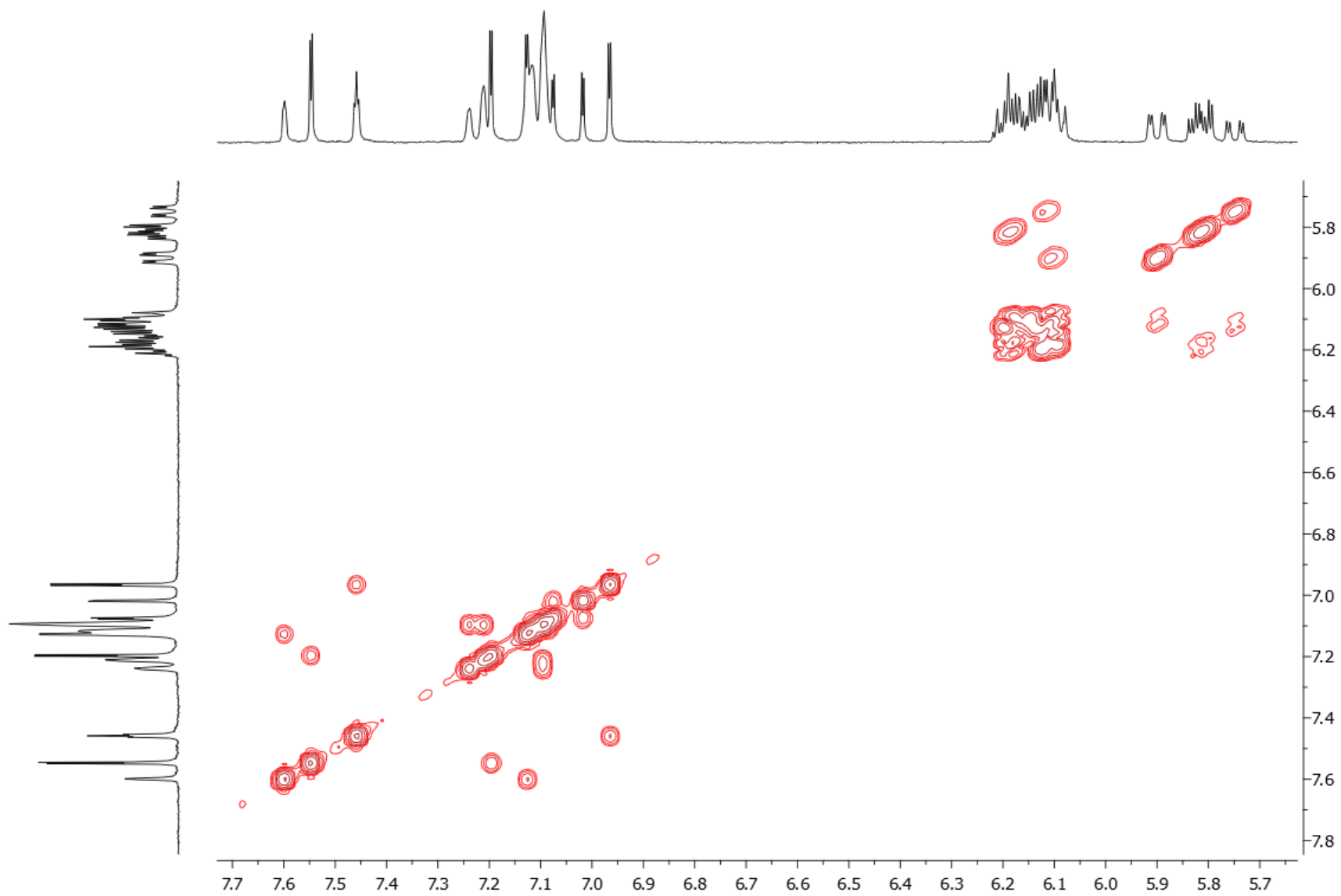
**Spectrum S13.** <sup>1</sup>H NMR spectrum (700 MHz) of **7** in CD<sub>2</sub>Cl<sub>2</sub> (TMS).



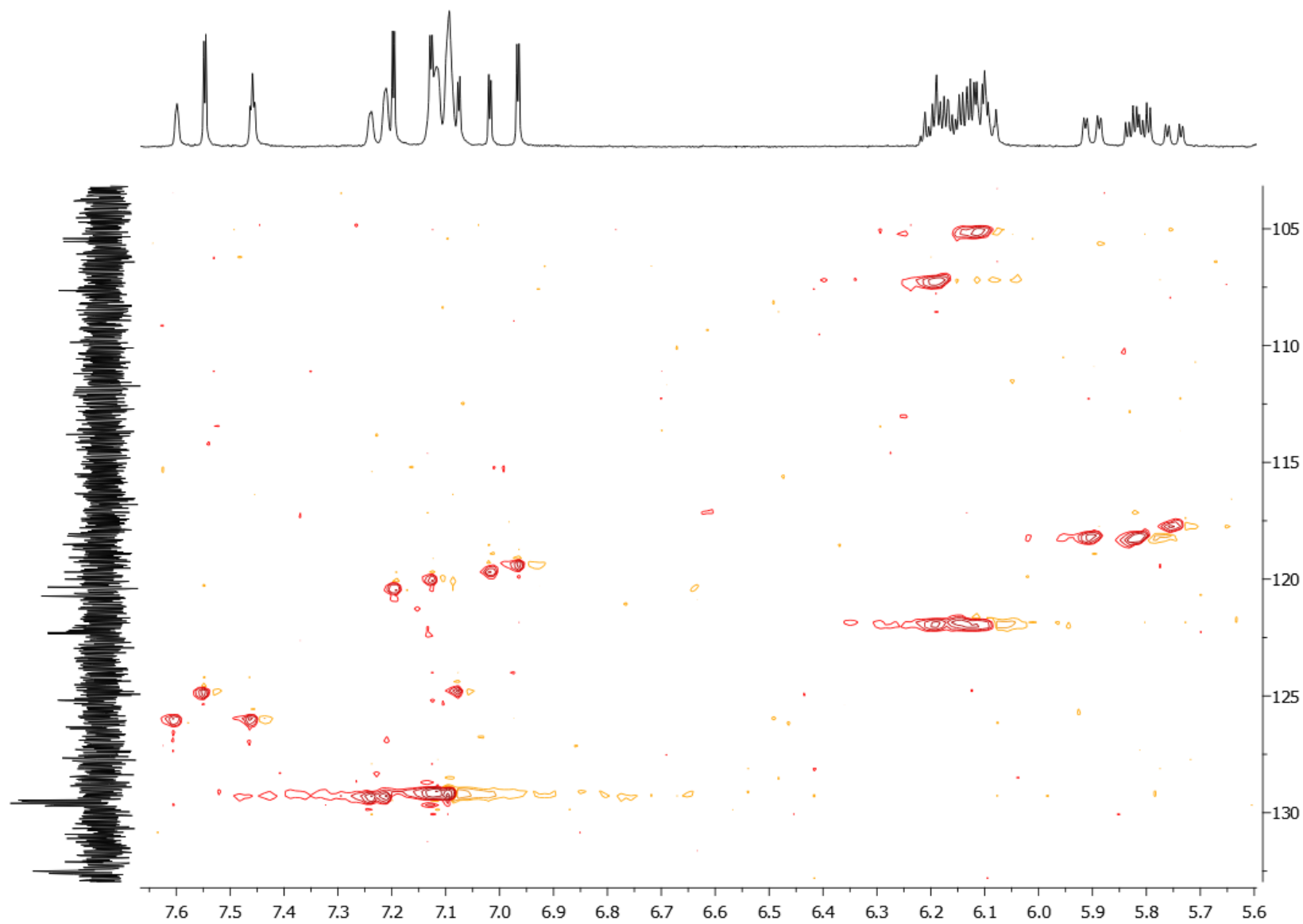
**Spectrum S14.**  $^{19}\text{F}\{^1\text{H}\}$  NMR spectrum (376 MHz) of **7** in  $\text{CD}_2\text{Cl}_2$ .



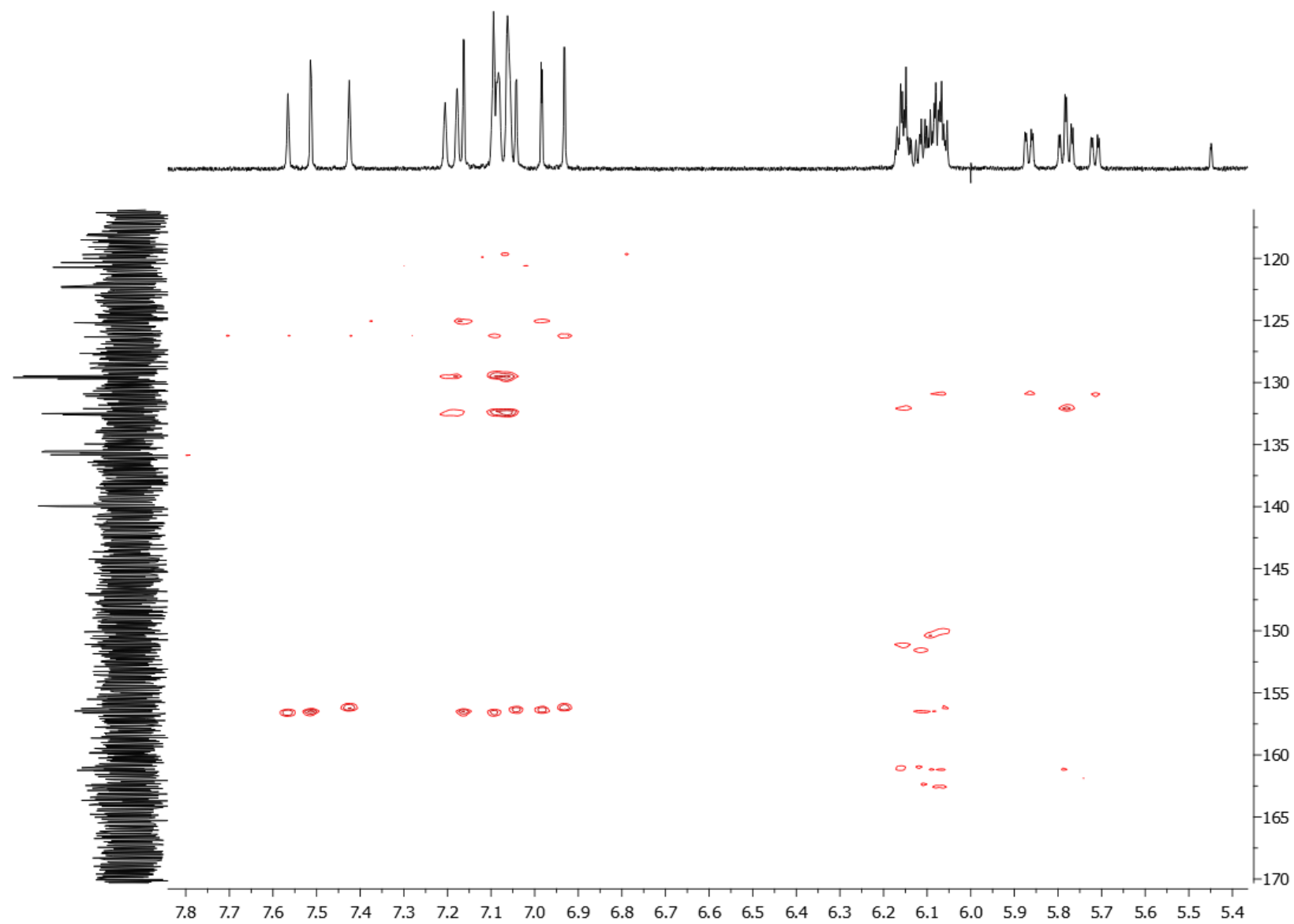
**Spectrum S15.**  $^{13}\text{C}$  NMR spectrum (151 MHz) of **7** in  $\text{CD}_2\text{Cl}_2$  (TMS).



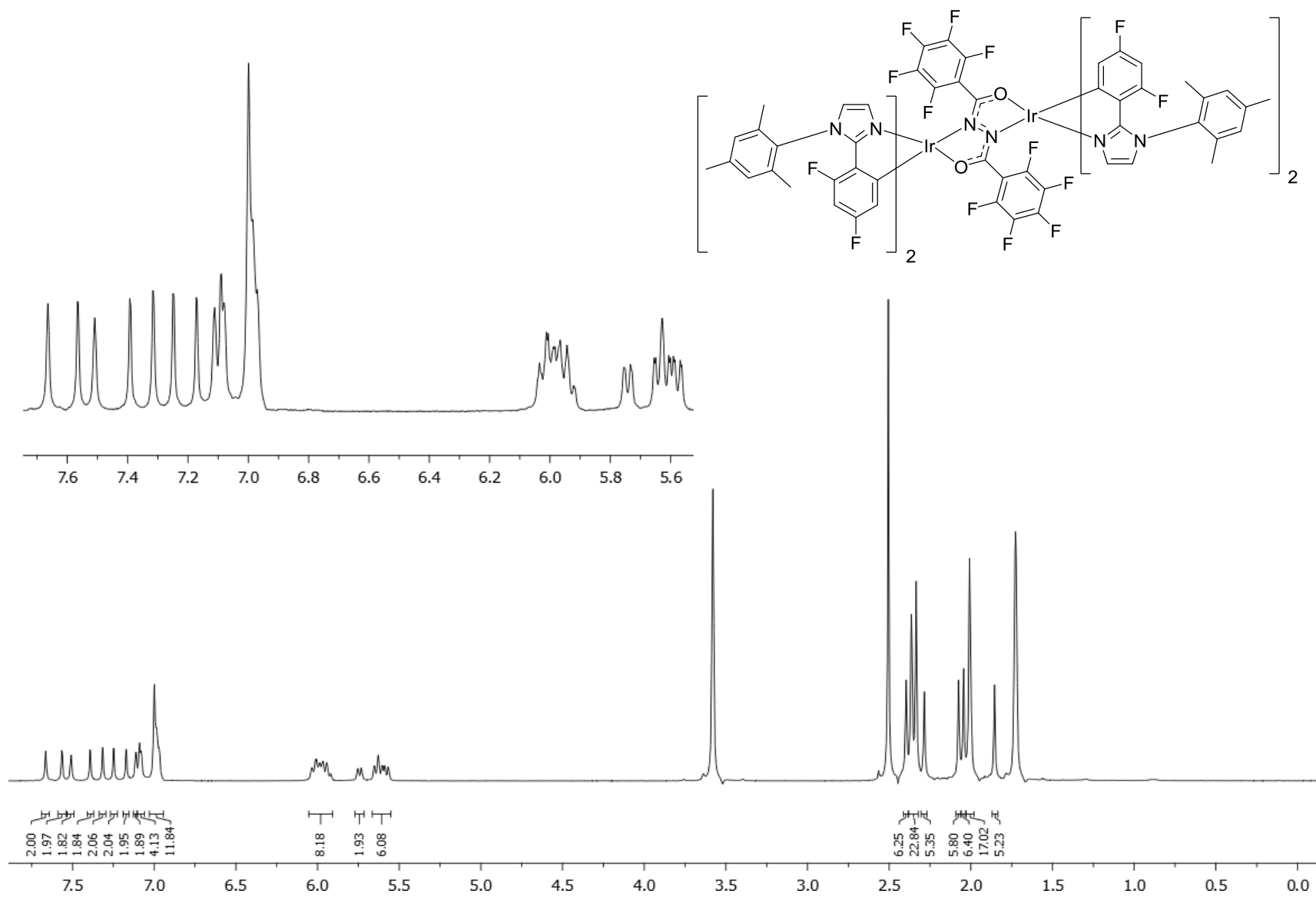
**Spectrum S16.** Expansion of the aromatic region of the  $^1\text{H}$ - $^1\text{H}$  COSY NMR spectrum of **7** in  $\text{CD}_2\text{Cl}_2$  (TMS).



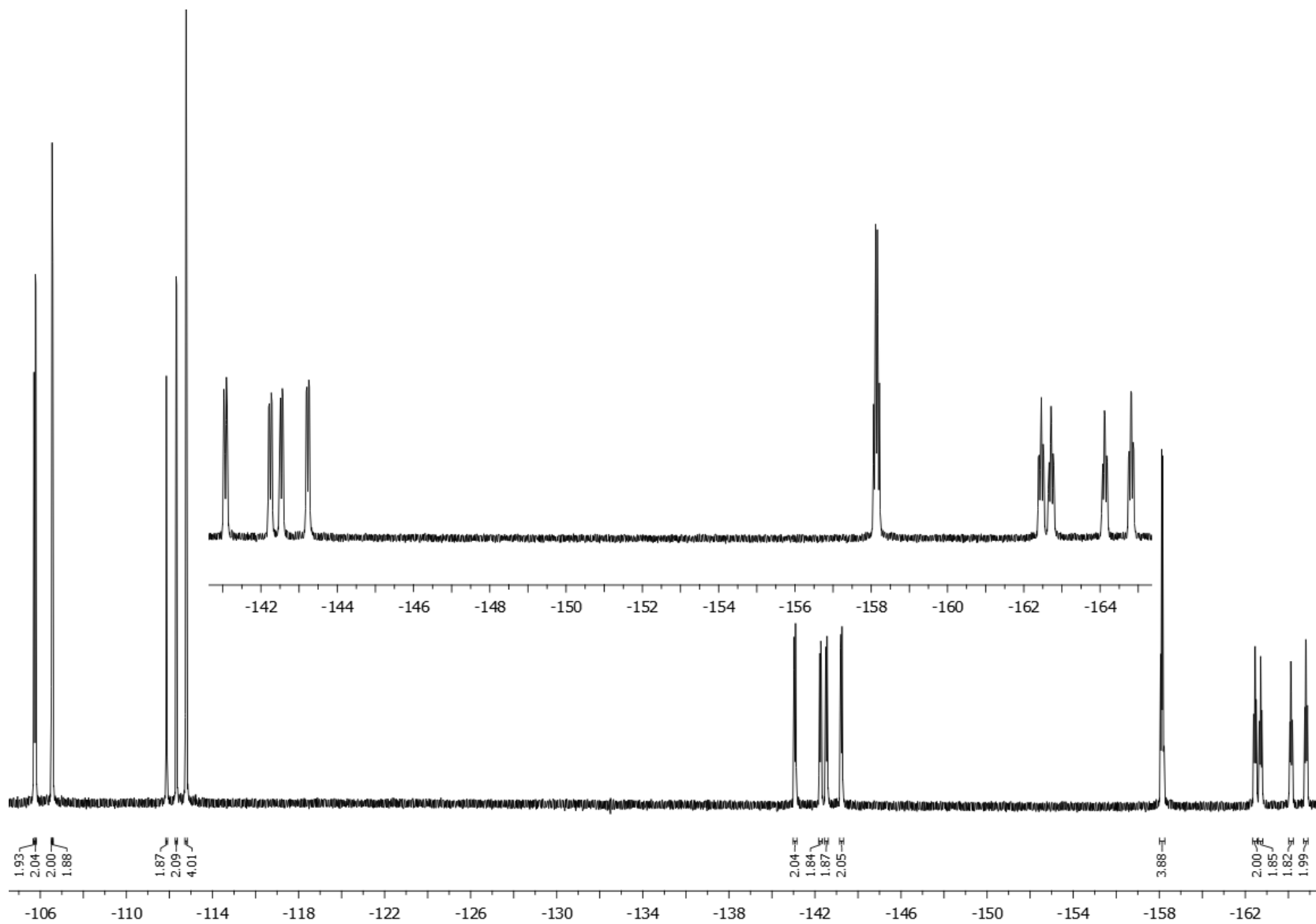
**Spectrum S17.** Expansion of the aromatic region of the  $^1\text{H}$ - $^{13}\text{C}$  HSQC NMR spectrum of **7** in  $\text{CD}_2\text{Cl}_2$  (TMS).



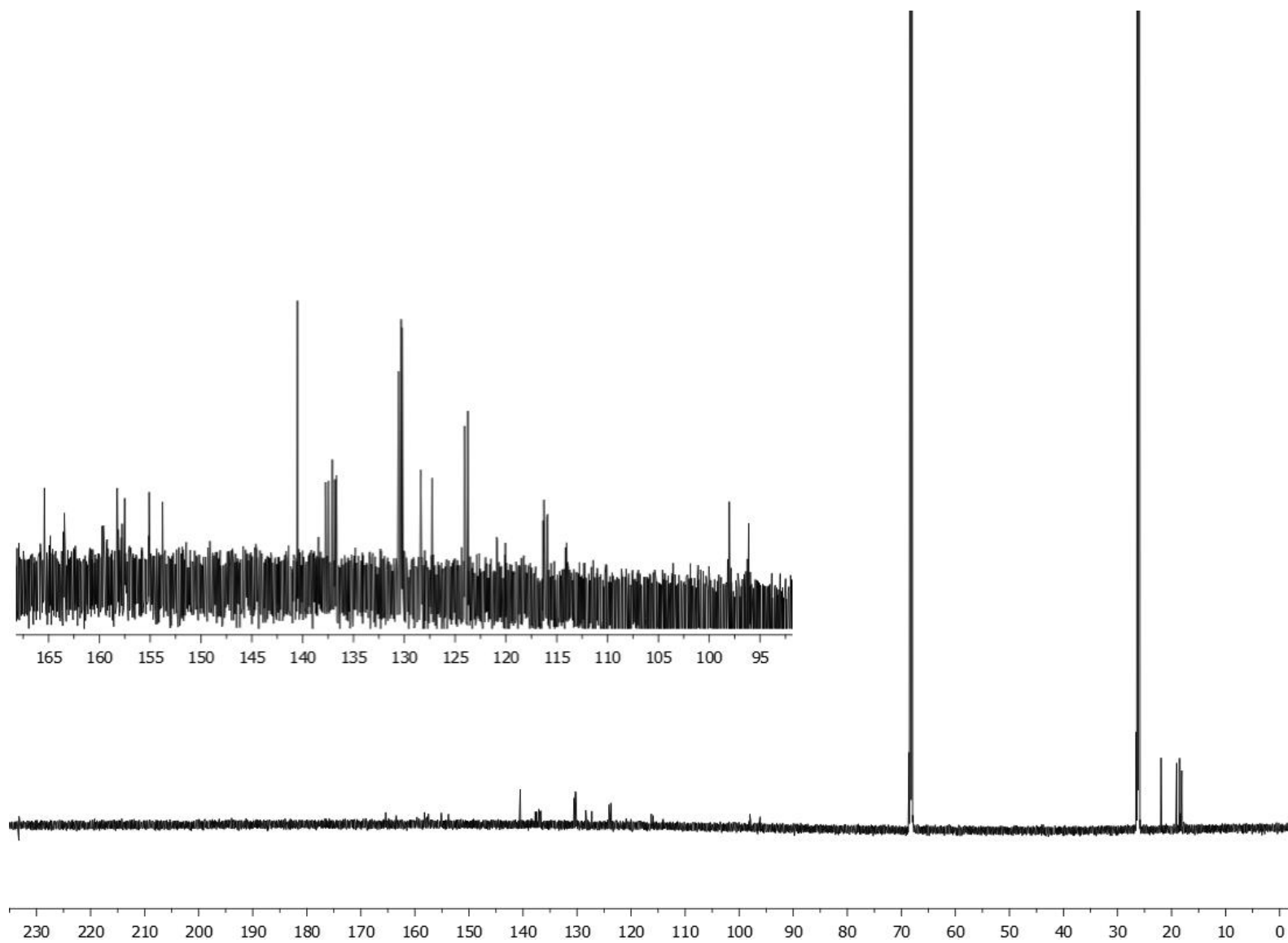
**Spectrum S18.** Expansion of the aromatic region of the  $^1\text{H}$ - $^{13}\text{C}$  HMBC NMR spectrum of **7** in  $\text{CD}_2\text{Cl}_2$  (TMS).



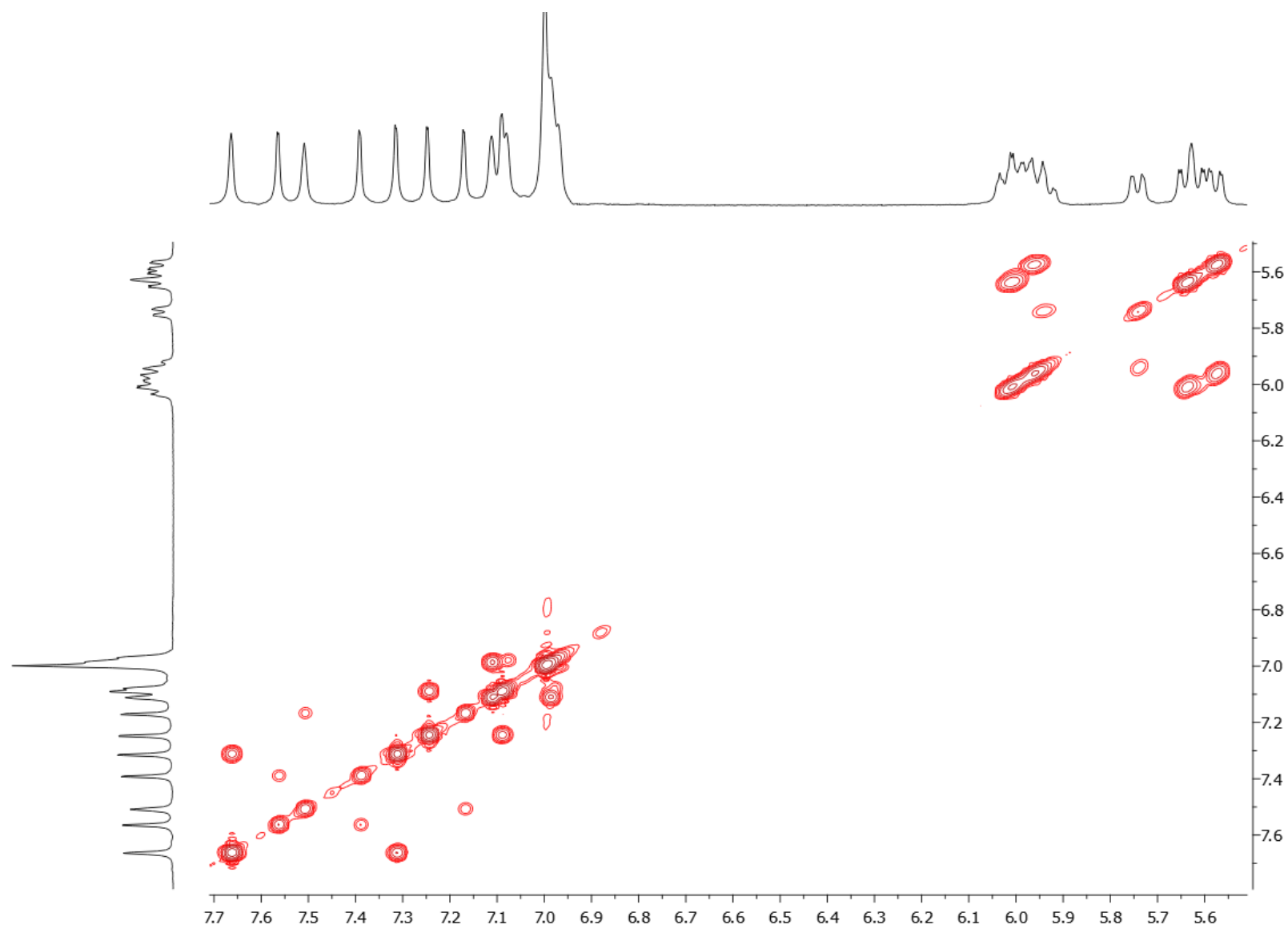
**Spectrum S19.**  $^1\text{H}$  NMR spectrum (700 MHz) of **8** in  $\text{D}_8\text{-THF}$ .



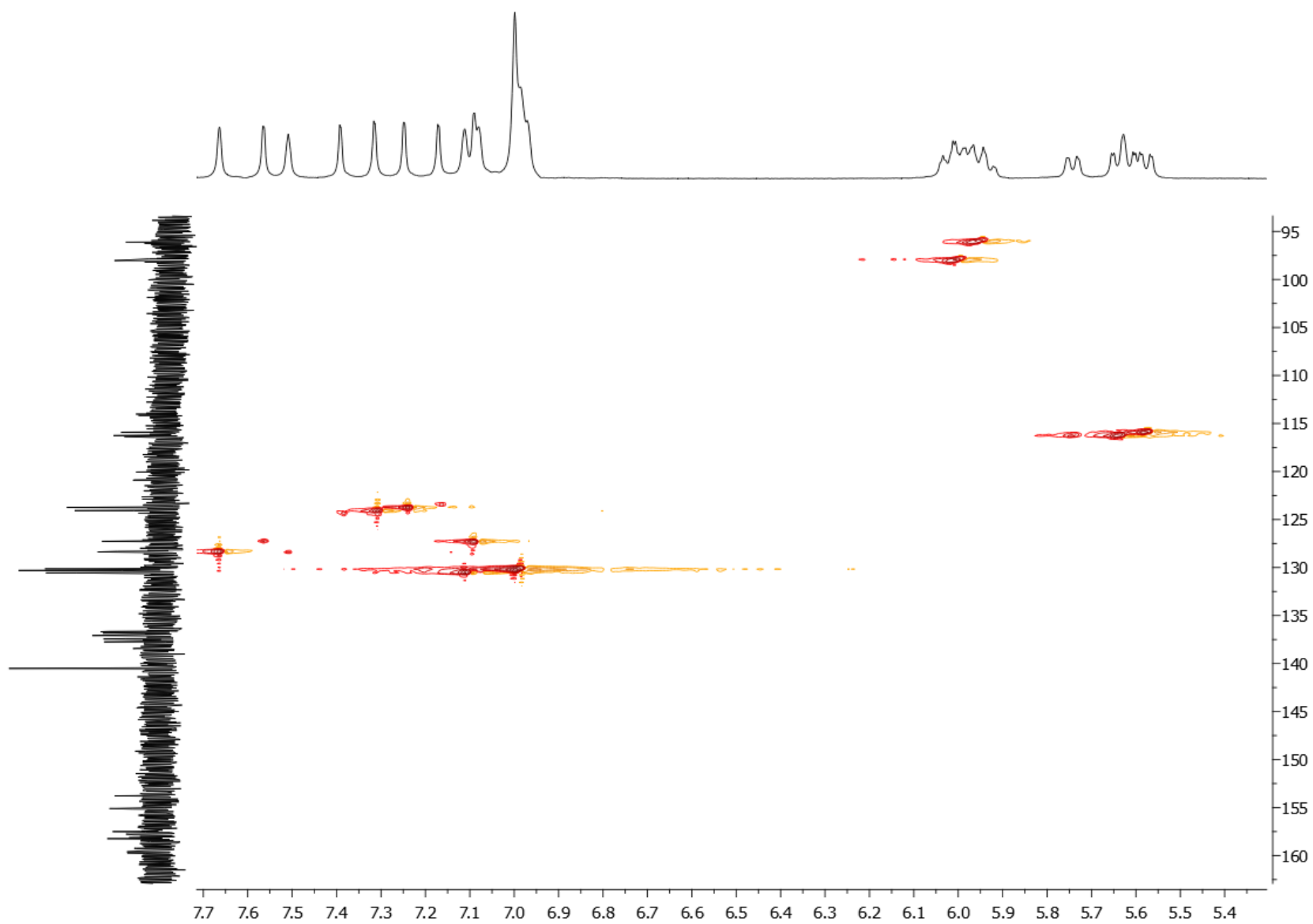
**Spectrum S20.**  $^{19}\text{F}\{^1\text{H}\}$  NMR spectrum (376 MHz) of **8** in  $\text{D}_8\text{-THF}$ .



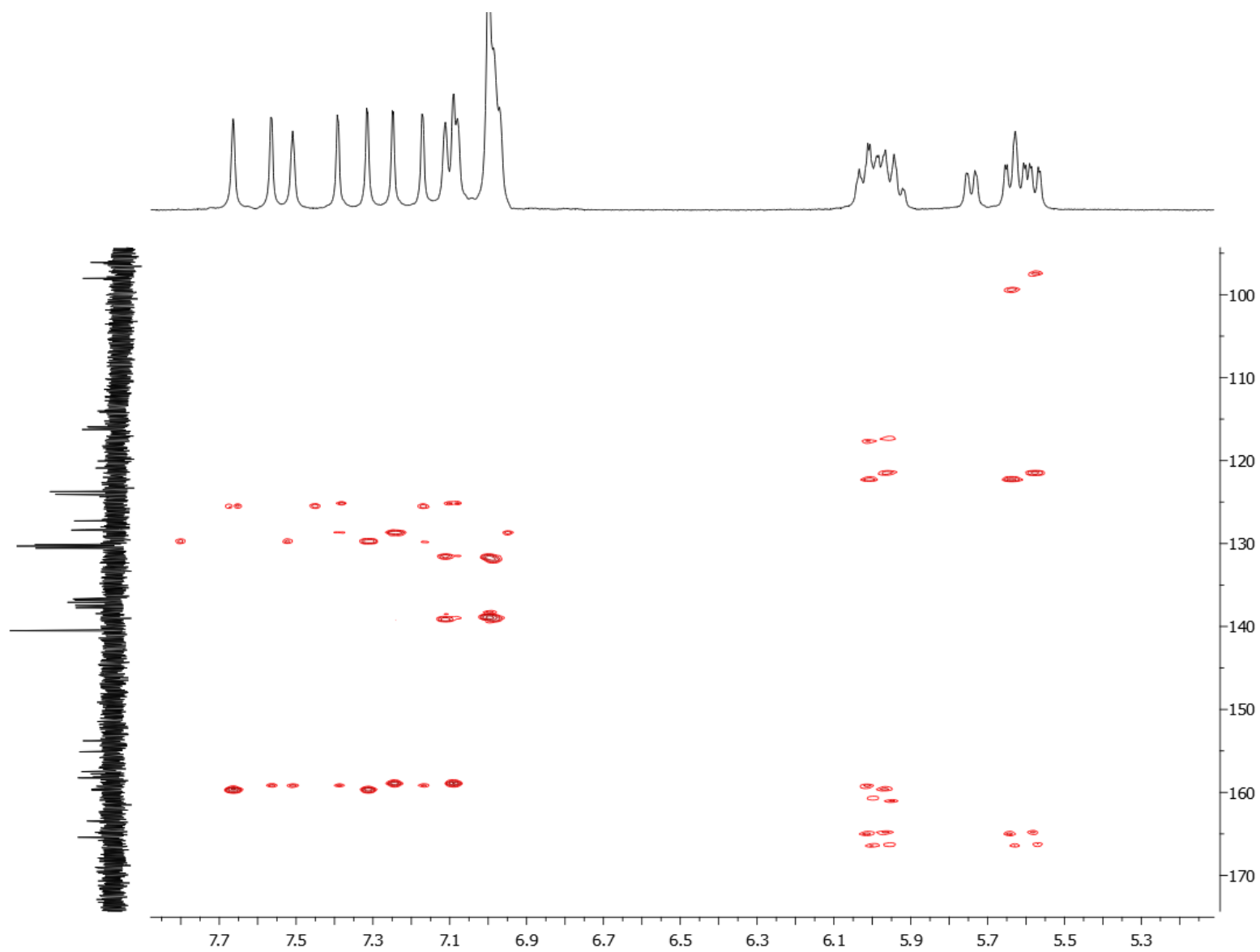
**Spectrum S21.**  $^{13}\text{C}$  NMR spectrum (151 MHz) of **8** in  $\text{D}_8\text{-THF}$ .



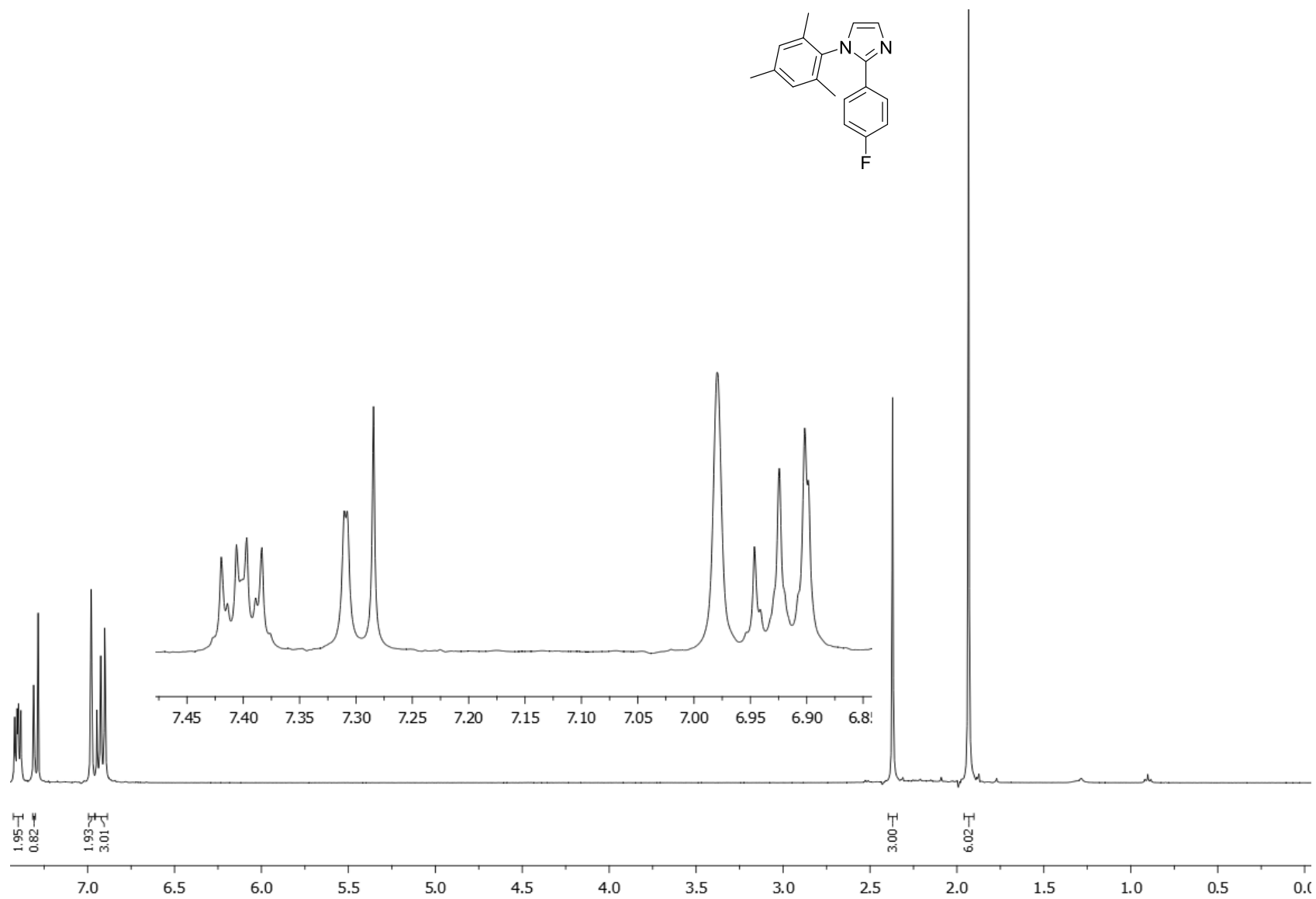
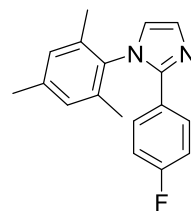
**Spectrum S22.** Expansion of the aromatic region of the  $^1\text{H}$ - $^1\text{H}$  COSY NMR spectrum of **8** in  $\text{D}_8$ -THF.



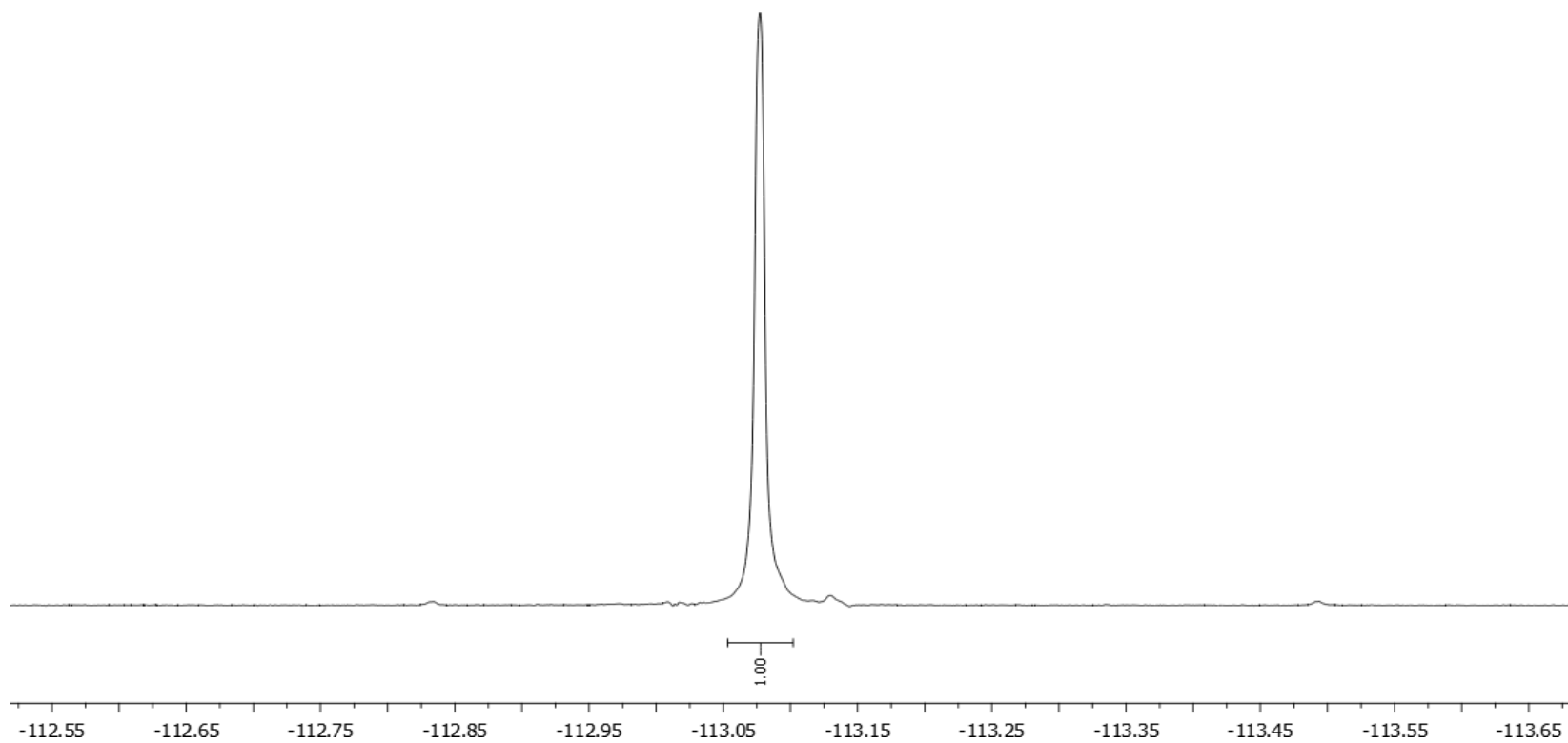
**Spectrum S23.** Expansion of the aromatic region of the  $^1\text{H}$ - $^{13}\text{C}$  HSQC NMR spectrum of **8** in  $\text{D}_8$ -THF.



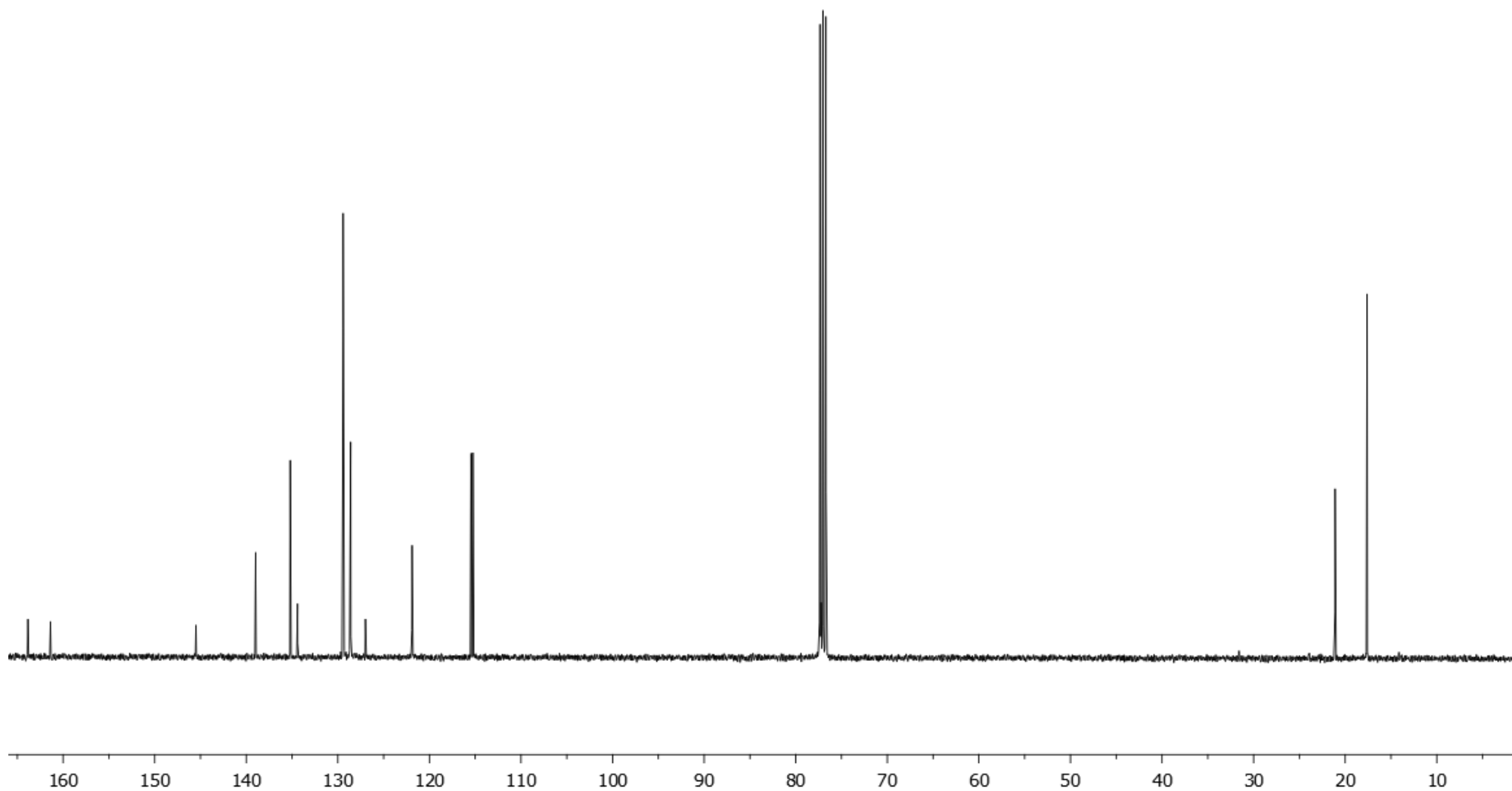
**Spectrum S24.** Expansion of the aromatic region of the  $^1\text{H}$ - $^{13}\text{C}$  HMBC NMR spectrum of **8** in  $\text{D}_8$ -THF.



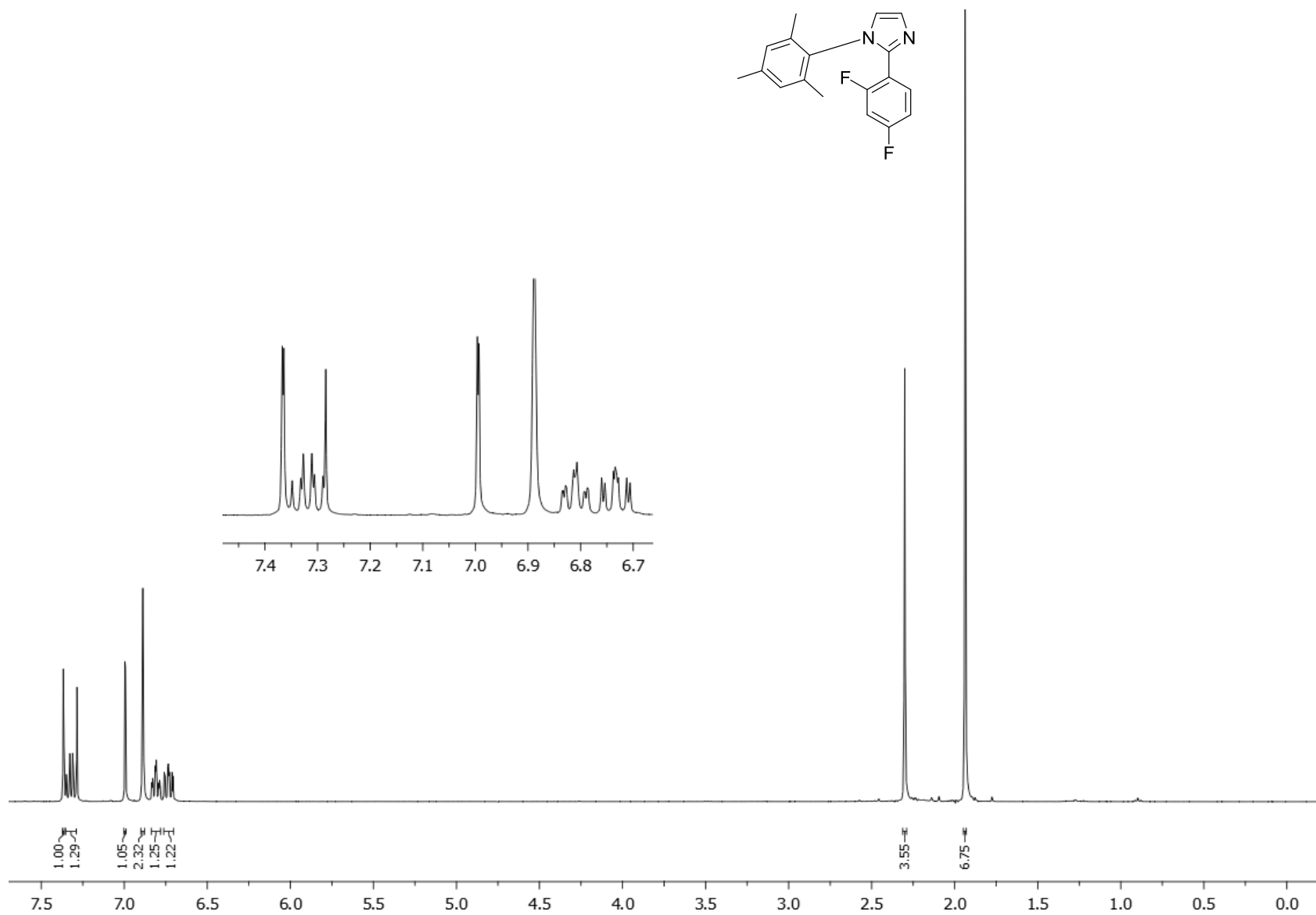
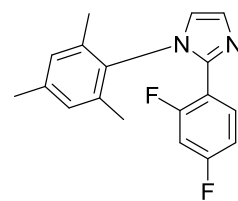
**Spectrum S25.**  $^1\text{H}$  NMR spectrum (400 MHz) of H10 in  $\text{CDCl}_3$ .



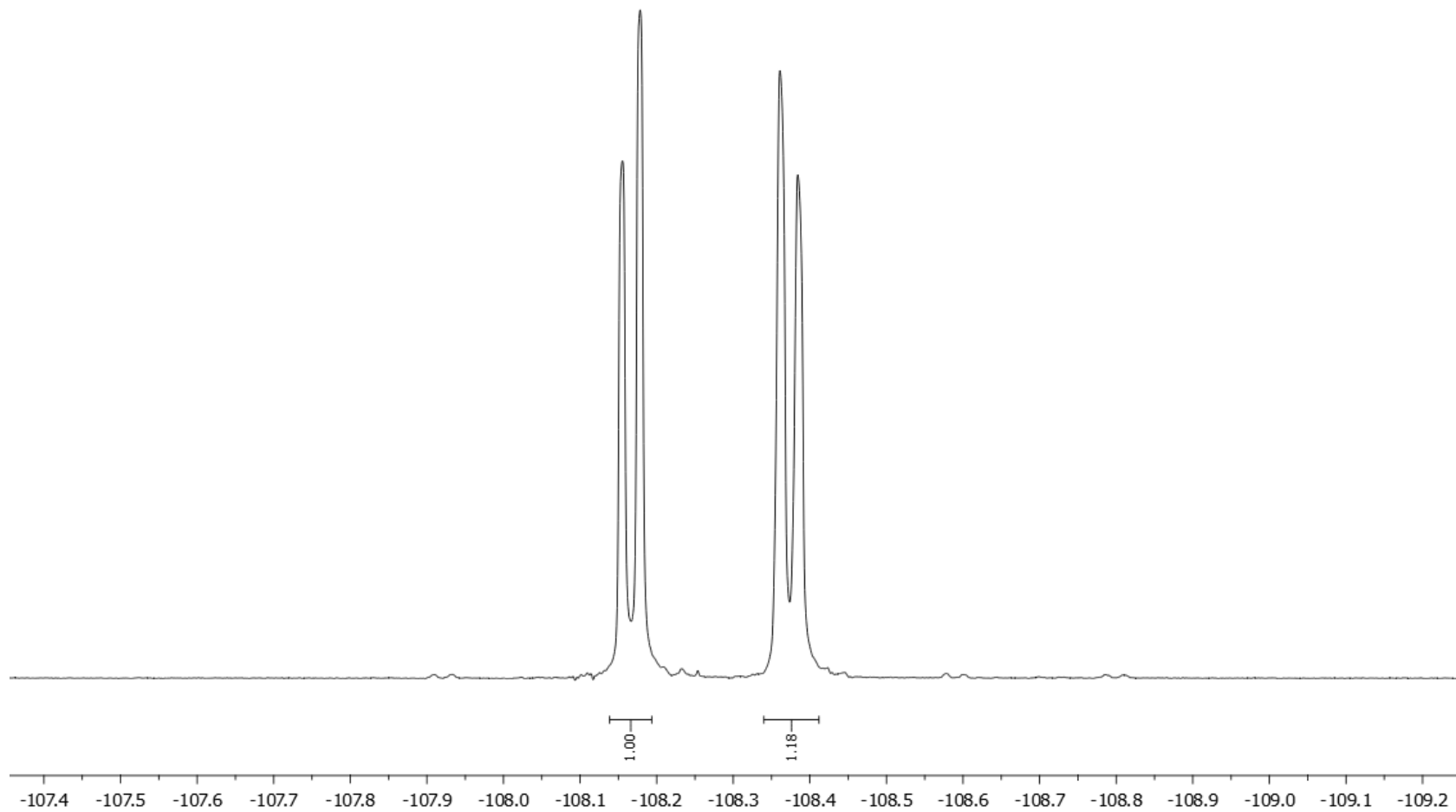
**Spectrum S26.**  $^{19}\text{F}\{^1\text{H}\}$  NMR spectrum (376 MHz) of H10 in  $\text{CDCl}_3$ .



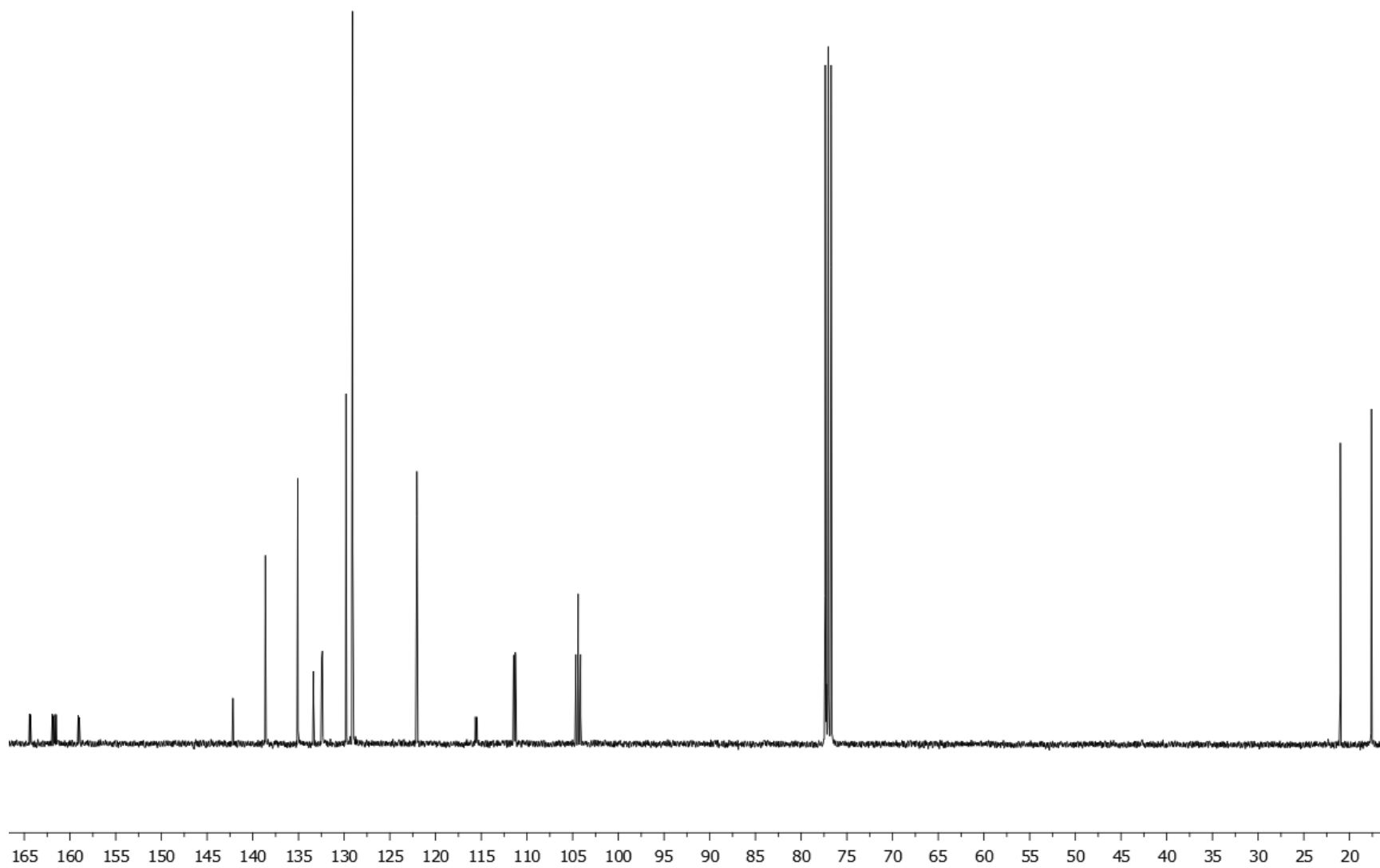
**Spectrum S27.**  $^{13}\text{C}$  NMR spectrum (101 MHz) of **H10** in  $\text{CDCl}_3$ .



**Spectrum S28.** <sup>1</sup>H NMR spectrum (400 MHz) of H11 in CDCl<sub>3</sub>.



**Spectrum S29.**  $^{19}\text{F}\{^1\text{H}\}$  NMR spectrum (376 MHz) of H11 in  $\text{CDCl}_3$ .



**Spectrum S30.**  $^{13}\text{C}$  NMR spectrum (101 MHz) of **H11** in  $\text{CDCl}_3$ .

## Electrochemistry

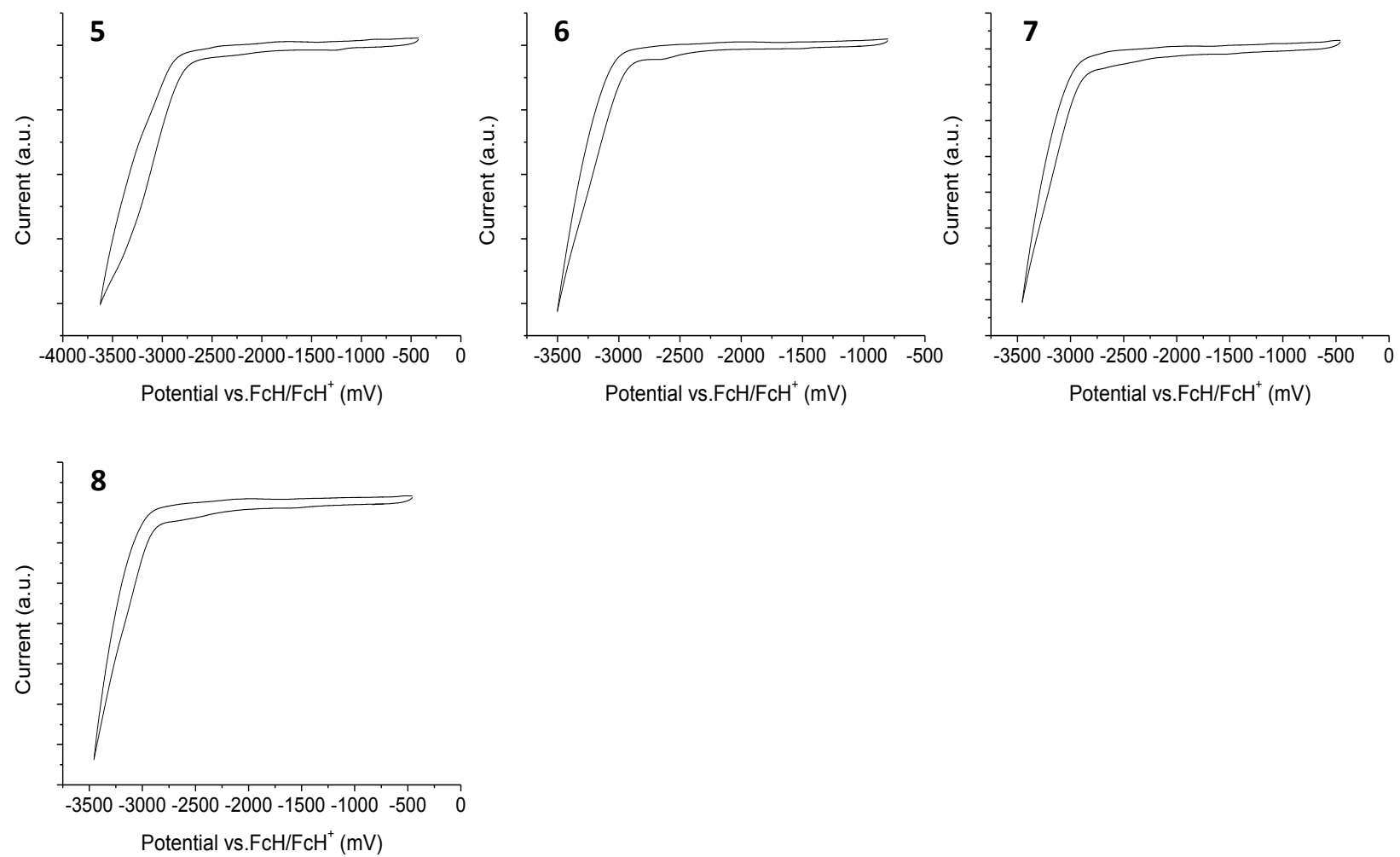


**Figure S1.** Cyclic voltammograms in 0.1 M *n*-Bu<sub>4</sub>PF<sub>6</sub>/ THF showing the reduction process for complexes 5-8.

## Photophysics

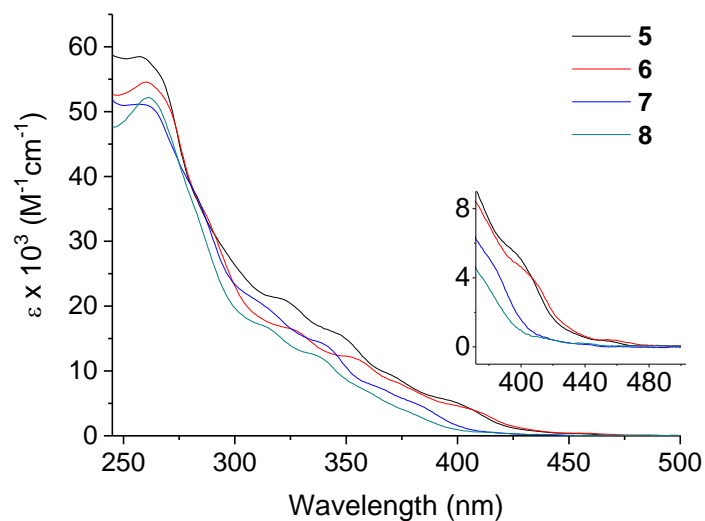


**Figure S2.** Absorption spectra for complexes **5–8** recorded in aerated DCM at room temperature.

**Table S1.** Tabulated absorption data for complexes **5–8** recorded in aerated DCM at room temperature.

Complex	$\lambda_{\text{abs}} / \text{nm}$ ( $\epsilon \times 10^3 / \text{M}^{-1} \text{cm}^{-1}$ )
<b>5</b>	258 (59), 288sh (34), 323 (21), 349 (16), 372 (9), 402 (5), 457 (0.3)
<b>6</b>	260 (55), 287sh (34), 327 (16), 355 (12), 378sh (7.6), 459 (0.4)
<b>7</b>	260 (51), 284sh (36), 315sh (20), 340 (14), 365sh (7.6), 384 (4.6), 442 (0.1)
<b>8</b>	261 (52), 283sh (33), 315 (17), 338 (12), 360sh (6.9), 379sh (3.4), 443 (0.2)

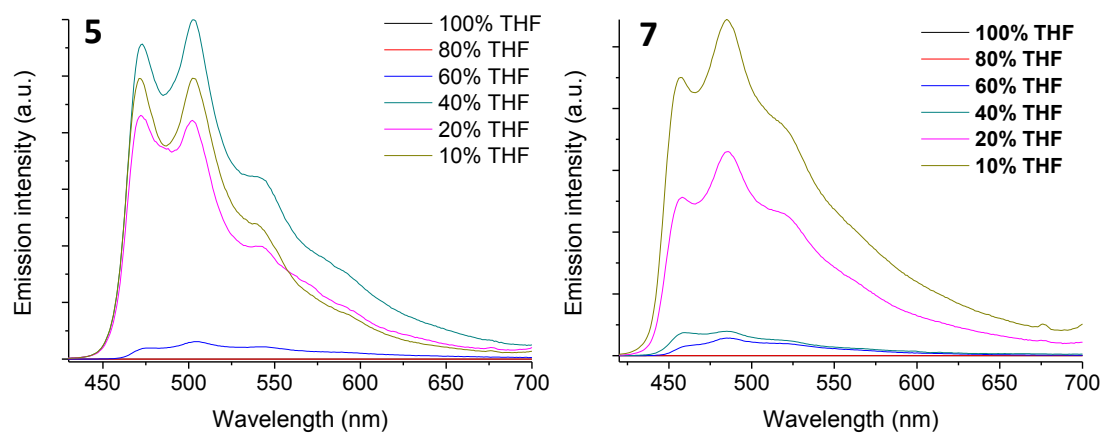


**Figure S3.** Emission spectra for THF solutions of complexes **5** and **7** upon incremental titration of water to induce precipitation ( $\lambda_{\text{exc}} 355 \text{ nm}$ ). THF fraction is percentage volume.

## Computations

Table S2. Summary of the orbital contributions for complexes 5–7.

Complex	Isomer	Orbital	Ir	Bridge centre	Ph <sup>a</sup>	Im <sup>b</sup>	Complex	Isomer	Orbital	Ir	Bridge centre	Bridge aryl	Ph <sup>a</sup>	Im <sup>b</sup>	Complex	Isomer	Orbital	Ir	Bridge centre	Bridge aryl	Ph <sup>a</sup>	Im <sup>b</sup>
5	<i>meso</i>	LUMO+5	3%	7%	35%	36%	6	<i>meso</i>	LUMO+5	1%	0%	10%	11%	13%	7	<i>meso</i>	LUMO+5	2%	1%	16%	26%	27%
		LUMO+4	0%	4%	4%	6%			LUMO+4	2%	1%	4%	29%	28%			LUMO+4	2%	1%	5%	36%	36%
		LUMO+3	1%	5%	4%	6%			LUMO+3	3%	3%	30%	34%	27%			LUMO+3	1%	1%	13%	45%	38%
		LUMO+2	3%	17%	28%	28%			LUMO+2	1%	1%	18%	42%	36%			LUMO+2	3%	2%	22%	38%	32%
		LUMO+1	3%	4%	43%	42%			LUMO+1	4%	2%	57%	19%	17%			LUMO+1	4%	3%	68%	13%	12%
		LUMO	3%	1%	49%	44%			LUMO	2%	7%	58%	17%	16%			LUMO	1%	9%	67%	11%	11%
	HOMO	45%	14%	33%	8%	HOMO	44%	41%	1%	7%	7%	HOMO	43%	43%	1%	6%	7%					
	HOMO-1	47%	2%	40%	10%	HOMO-1	47%	7%	0%	37%	8%	HOMO-1	46%	5%	0%	38%	10%					
	HOMO-2	48%	31%	13%	8%	HOMO-2	47%	2%	1%	40%	10%	HOMO-2	45%	2%	1%	38%	14%					
	HOMO-3	63%	6%	18%	13%	HOMO-3	65%	7%	0%	14%	14%	HOMO-3	50%	4%	1%	23%	22%					
	HOMO-4	45%	4%	28%	23%	HOMO-4	45%	4%	1%	25%	25%	HOMO-4	48%	5%	1%	27%	19%					
	HOMO-5	43%	3%	29%	25%	HOMO-5	60%	5%	1%	16%	19%	HOMO-5	55%	5%	1%	20%	19%					
	LUMO+5	1%	0%	6%	94%	LUMO+5	2%	2%	16%	25%	54%	LUMO+5	3%	1%	5%	39%	36%					
	LUMO+4	1%	1%	6%	93%	LUMO+4	2%	0%	6%	32%	59%	LUMO+4	2%	2%	9%	36%	35%					
	LUMO+3	1%	0%	8%	92%	LUMO+3	2%	3%	40%	28%	26%	LUMO+3	3%	2%	24%	37%	31%					
LUMO+2	1%	1%	14%	84%	LUMO+2	3%	3%	74%	10%	11%	LUMO+2	2%	2%	4%	47%	41%						
LUMO+1	3%	1%	44%	52%	LUMO+1	2%	1%	1%	49%	46%	LUMO+1	3%	4%	78%	8%	7%						
LUMO	2%	1%	43%	53%	LUMO	2%	3%	50%	23%	22%	LUMO	1%	4%	67%	14%	13%						
HOMO	46%	34%	13%	7%	HOMO	44%	40%	1%	8%	7%	HOMO	43%	42%	1%	7%	7%						
HOMO-1	49%	4%	40%	8%	HOMO-1	50%	3%	0%	38%	8%	HOMO-1	48%	3%	0%	37%	11%						
HOMO-2	42%	13%	35%	10%	HOMO-2	44%	8%	0%	38%	10%	HOMO-2	41%	6%	0%	385	14%						
HOMO-3	64%	8%	14%	14%	HOMO-3	64%	9%	0%	13%	14%	HOMO-3	60%	8%	0%	16%	15%						
HOMO-4	40%	2%	31%	27%	HOMO-4	42%	2%	1%	28%	27%	HOMO-4	33%	2%	1%	35%	28%						
HOMO-5	61%	3%	19%	17%	HOMO-5	63%	2%	0%	17%	17%	HOMO-5	53%	2%	1%	26%	18%						

<sup>a</sup>Phenyl moieties of the cyclometalating ligands. <sup>b</sup>Imidazole moieties of the cyclometalating ligands.

**Table S3.** Summary of the orbital contributions for complex **8**.

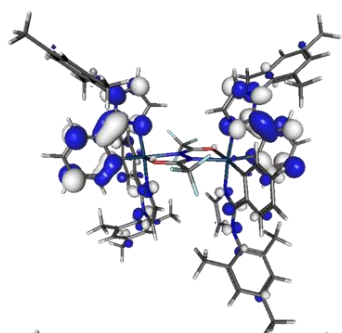
Complex	Isomer	Orbital	Ir	Bridge centre	Bridge aryl	Ph <sup>a</sup>	Im <sup>b</sup>
<b>8</b>	<i>meso</i>	LUMO+5	3%	1%	25%	36%	33%
		LUMO+4	4%	1%	1%	48%	44%
		LUMO+3	3%	3%	31%	34%	28%
		LUMO+2	1%	1%	18%	42%	36%
		LUMO+1	4%	2%	53%	21%	19%
		LUMO	2%	8%	56%	17%	17%
		HOMO	42%	45%	1%	5%	8%
		HOMO-1	47%	4%	0%	37%	11%
		HOMO-2	47%	3%	1%	35%	15%
		HOMO-3	47%	4%	1%	25%	24%
	HOMO-4	47%	5%	1%	27%	19%	
	HOMO-5	49%	4%	1%	26%	20%	
	<i>rac</i>	LUMO+5	3%	3%	22%	37%	33%
		LUMO+4	4%	1%	10%	45%	38%
		LUMO+3	4%	2%	14%	41%	37%
		LUMO+2	3%	2%	2%	48%	43%
		LUMO+1	3%	2%	70%	13%	12%
		LUMO	1%	4%	71%	12%	11%
		HOMO	43%	44%	1%	6%	6%
		HOMO-1	50%	3%	0%	35%	12%
HOMO-2		41%	5%	1%	37%	17%	
HOMO-3		56%	8%	0%	21%	14%	
HOMO-4	33%	2%	1%	32%	32%		
HOMO-5	50%	2%	1%	31%	16%		

<sup>a</sup>Phenyl moieties of the cyclometalating ligands. <sup>b</sup>Imidazole moieties of the cyclometalating ligands.

**Table S4.** Summary of the TD-DFT data for complexes **5** and **7**.

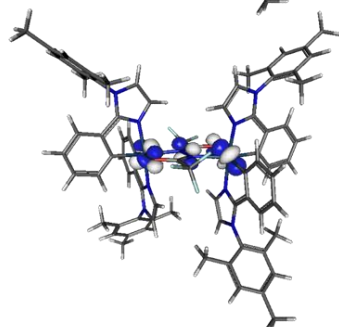
Transition	<b>5</b>				<b>7</b>			
	<i>meso</i>		<i>rac</i>		<i>meso</i>		<i>rac</i>	
	Main orbital contribution	$\lambda/\text{nm}$ (f)	Main orbital contribution	$\lambda/\text{nm}$ (f)	Main orbital contribution	$\lambda/\text{nm}$ (f)	Main orbital contribution	$\lambda/\text{nm}$ (f)
$S_0 \rightarrow T_1$	HOMO-2 $\rightarrow$ LUMO+6, HOMO-2 $\rightarrow$ LUMO+8	458	HOMO $\rightarrow$ LUMO+8	460	HOMO $\rightarrow$ LUMO	424	HOMO-1 $\rightarrow$ LUMO+3, HOMO $\rightarrow$ LUMO+2	415
$S_0 \rightarrow T_2$	HOMO $\rightarrow$ LUMO+1	425	HOMO-1 $\rightarrow$ LUMO+1, HOMO $\rightarrow$ LUMO	425	HOMO $\rightarrow$ LUMO+1, HOMO-2 $\rightarrow$ LUMO+2	415	HOMO-1 $\rightarrow$ LUMO+2, HOMO $\rightarrow$ LUMO+3	415
$S_0 \rightarrow T_3$	HOMO-1 $\rightarrow$ LUMO	422	HOMO-1 $\rightarrow$ LUMO, HOMO $\rightarrow$ LUMO+1	425	HOMO-2 $\rightarrow$ LUMO+3, HOMO $\rightarrow$ LUMO+2	404	HOMO $\rightarrow$ LUMO+1, HOMO $\rightarrow$ LUMO+16	411
$S_0 \rightarrow T_4$	HOMO $\rightarrow$ LUMO+5, HOMO $\rightarrow$ LUMO+8	417	HOMO-1 $\rightarrow$ LUMO+2	416	HOMO-2 $\rightarrow$ LUMO+3, HOMO-1 $\rightarrow$ LUMO+4	406	HOMO-1 $\rightarrow$ LUMO+2, HOMO-1 $\rightarrow$ LUMO+4	407
$S_0 \rightarrow T_5$	HOMO-1 $\rightarrow$ LUMO+2	414	HOMO-2 $\rightarrow$ LUMO+2, HOMO-1 $\rightarrow$ LUMO+7	416	HOMO-2 $\rightarrow$ LUMO+4, HOMO-1 $\rightarrow$ LUMO+3	406	HOMO-2 $\rightarrow$ LUMO+2, HOMO-1 $\rightarrow$ LUMO+5	407

*rac 5*



LUMO  
-0.54 eV

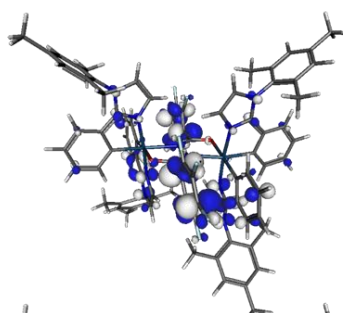
Ir : Bridge : Ph : Im  
2 : 1 : 43 : 53



HOMO  
-4.38 eV

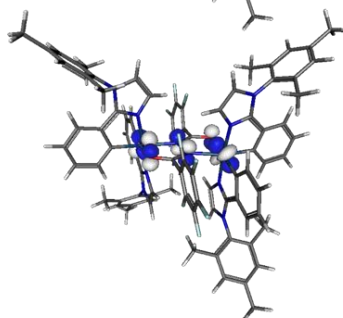
Ir : Bridge : Ph : Py  
46 : 34 : 13 : 46

*rac 6*



LUMO  
-0.58 eV

Ir : Bridge : F<sub>3</sub> : Ph : Im  
2 : 3 : 50 : 23 : 22

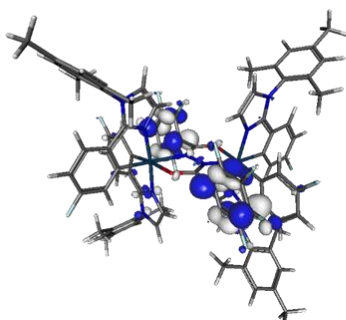


HOMO  
-4.45 eV

Ir : Bridge : F<sub>3</sub> : Ph : Im  
44 : 40 : 1 : 8 : 7

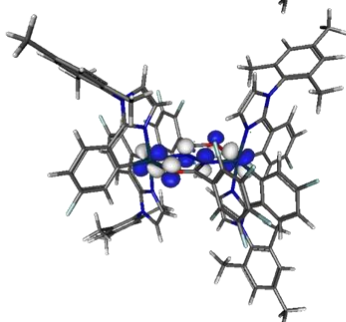
Figure S4. Frontier molecular orbitals for the most stable minima of *rac 5* and *rac 6*.

*rac 7*



LUMO  
-0.73 eV

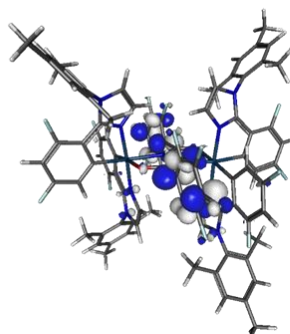
Ir : Bridge : F<sub>3</sub> : Ph : Im  
1 : 4 : 67 : 14 : 14



HOMO  
-4.68 eV

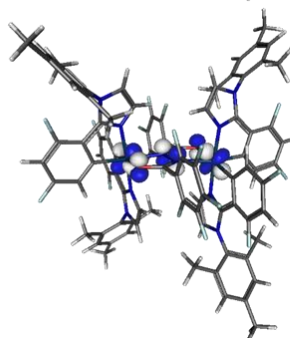
Ir : Bridge : F<sub>3</sub> : Ph : Im  
43 : 42 : 1 : 7 : 7

*rac 8*



LUMO  
-1.00 eV

Ir : Bridge : F<sub>3</sub> : Ph : Im  
1 : 4 : 71 : 12 : 11

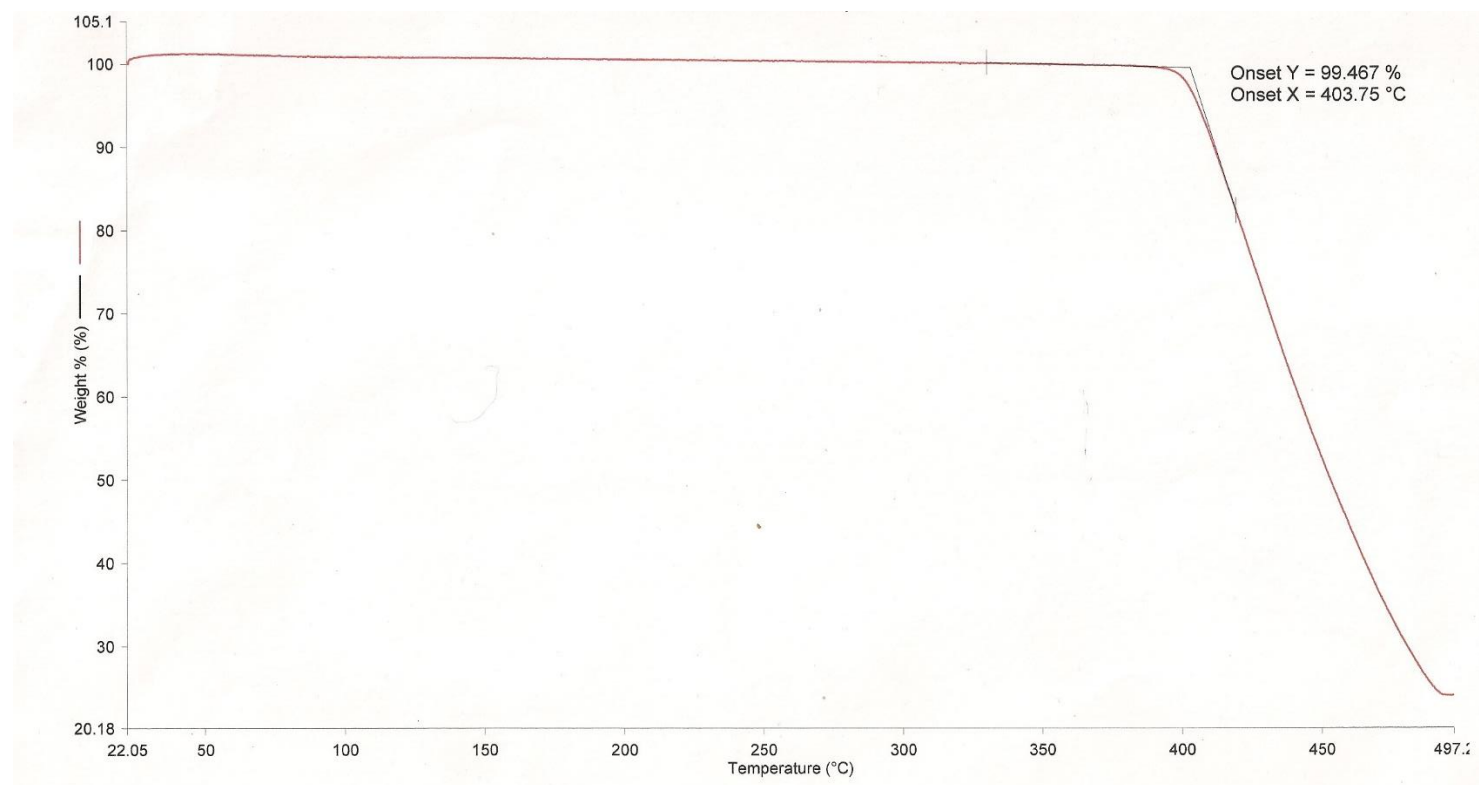


HOMO  
-5.08 eV

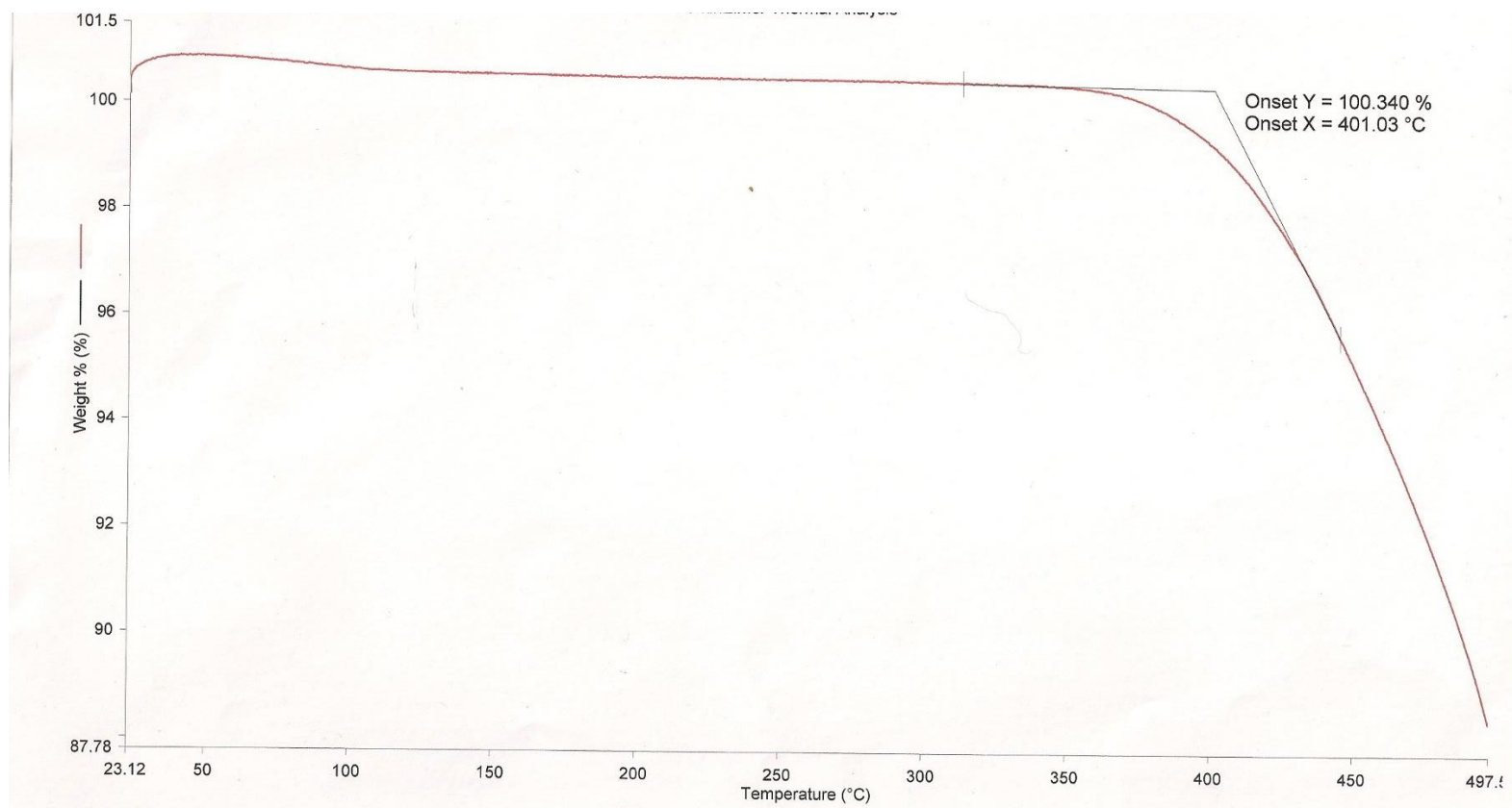
Ir : Bridge : F<sub>3</sub> : Ph : Im  
43 : 44 : 1 : 6 : 6

Figure S5. Frontier molecular orbitals for the most stable minima of *rac 7* and *rac 8*

## Thermal Analysis



**Figure S6.** TGA trace for complex 5. Onset = 404 °C



**Figure S7.** TGA trace for complex **6**. Onset = 401 °C

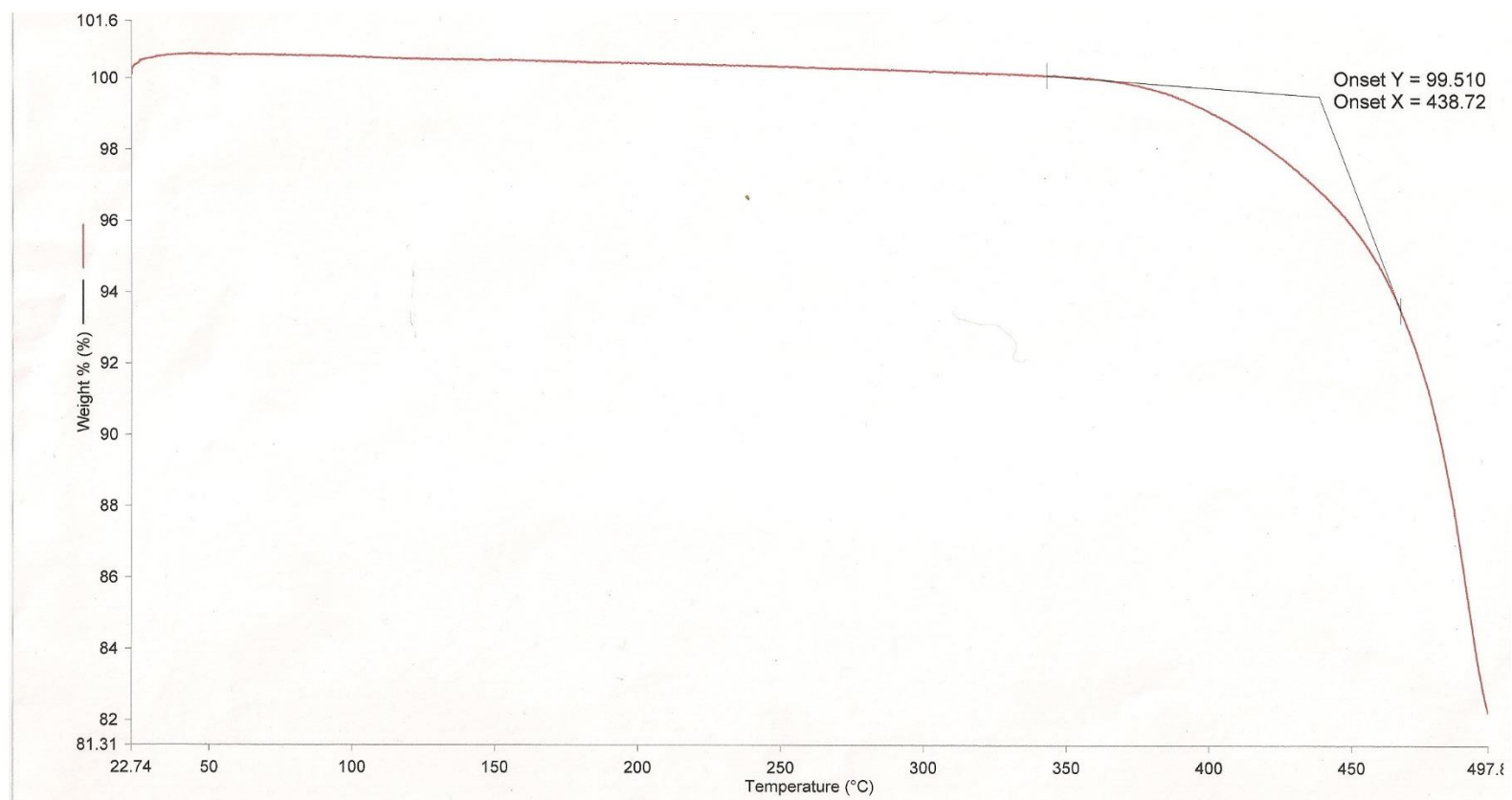


**Figure S8.** TGA trace for complex 7. Onset = 439 °C

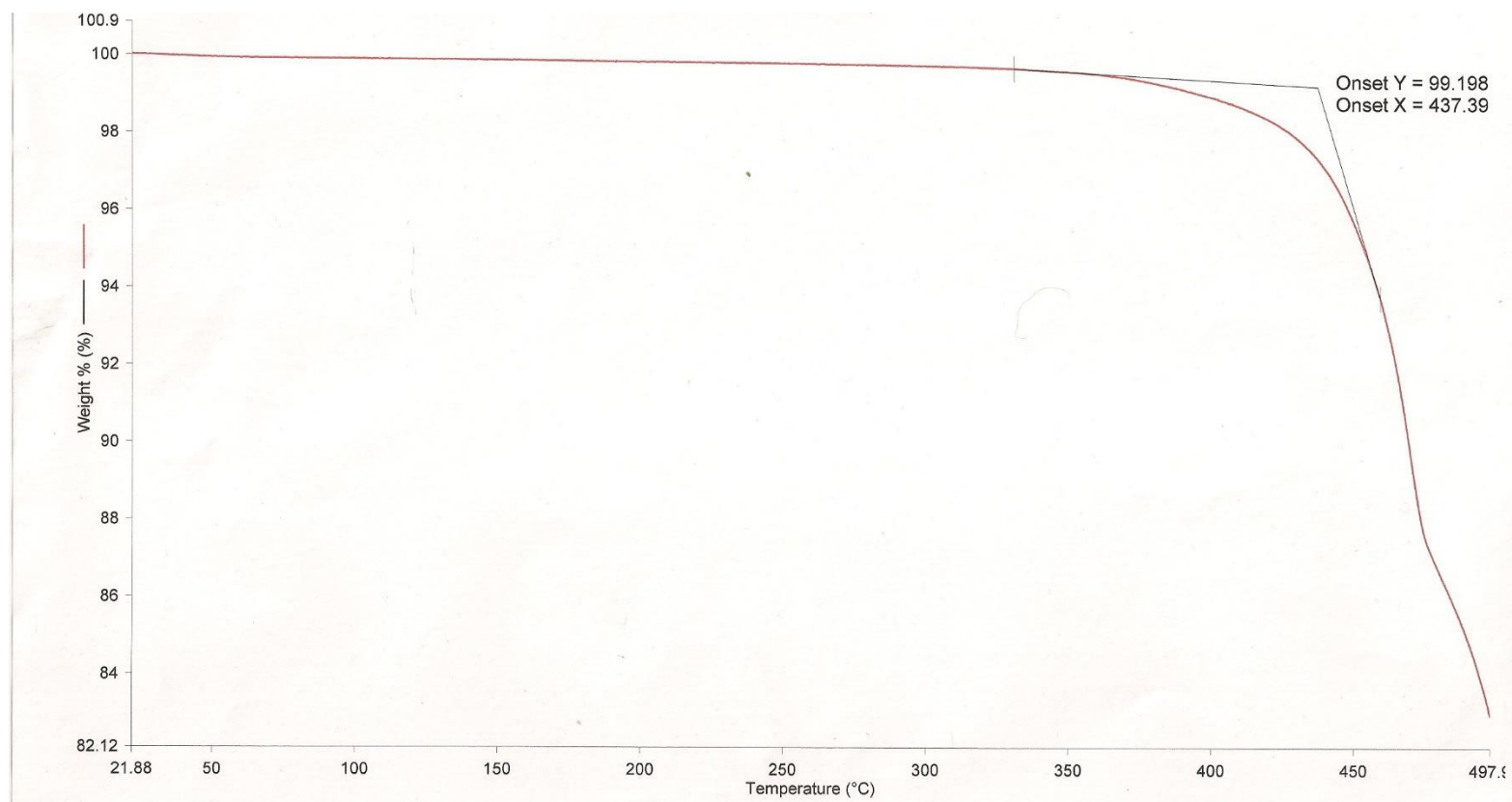


**Figure S9.** TGA trace for complex **8**. Onset = 437 °C.

## X-ray crystallography

Table S5. Crystal data

Compound	<i>meso-7</i>	<i>meso-8</i>
CCDC dep. no.	1871136	1871137
Formula	C <sub>86</sub> H <sub>64</sub> F <sub>14</sub> Ir <sub>2</sub> N <sub>10</sub> O <sub>2</sub> ·6CH <sub>2</sub> Cl <sub>2</sub>	C <sub>86</sub> H <sub>60</sub> F <sub>18</sub> Ir <sub>2</sub> N <sub>10</sub> O <sub>2</sub> ·2MeOH
$D_{calc.}/\text{g cm}^{-3}$	1.706	1.687
$\mu/\text{mm}^{-1}$	3.232	3.385
Formula Weight	2429.42	2055.92
Size/mm <sup>3</sup>	0.25×0.07×0.06	0.44×0.25×0.12
<i>T</i> /K	120	120
Crystal System	monoclinic	orthorhombic
Space Group	<i>C2/c</i> (no. 15)	<i>Pbca</i> (no. 61)
<i>a</i> /Å	24.2045(10)	20.0605(10)
<i>b</i> /Å	14.8901(6)	13.1557(6)
<i>c</i> /Å	27.9788(12)	30.6755(15)
$\beta/^\circ$	110.265(2)	90
<i>V</i> /Å <sup>3</sup>	9459.6(7)	8095.6(7)
<i>Z</i>	4	4
$\Theta_{max}/^\circ$	30.000	32.575
Measured reflections	101919	175372
Unique reflections	13754	14709
Reflections with $I > 2\sigma(I)$	11072	11317
$R_{int}$	0.0520	0.0536
Parameters	616	576
Residual $\Delta\rho$ , eÅ <sup>-3</sup>	3.04, -1.45	3.66, -1.60
$R_1, wR_2 [I > 2\sigma(I)]$	0.0424, 0.1035	0.0378, 0.0738
$R_1, wR_2$ (all data)	0.0612, 0.1125	0.0610, 0.0813
Goodness of fit	1.079	1.077

## References

- 1 A. Fürstner, M. Alcarazo, V. César and C. W. Lehmann, *Chem. Commun.*, 2006, 2176–2178.
- 2 D. G. Congrave, Y.-T. Hsu, A. S. Batsanov, A. Beeby and M. R. Bryce, *Dalton Trans.*, 2018, **47**, 2086–2098.
- 3 Gaussian 09, Revision A.02, M. J. Frisch, G. W. Trucks, H. B. Schlegel, G. E. Scuseria, M. A. Robb, J. R. Cheeseman, G. Scalmani, V. Barone, B. Mennucci, G. A. Petersson, H. Nakatsuji, M. Caricato, X. Li, H. P. Hratchian, A. F. Izmaylov, J. Bloino, G. Zheng, J. L. Sonnenberg, M. Hada, M. Ehara, K. Toyota, R. Fukuda, J. Hasegawa, M. Ishida, T. Nakajima, Y. Honda, O. Kitao, H. Nakai, T. Vreven, J. A. Montgomery, Jr., J. E. Peralta, F. Ogliaro, M. Bearpark, J. J. Heyd, E. Brothers, K. N. Kudin, V. N. Staroverov, R. Kobayashi, J. Normand, K. Raghavachari, A. Rendell, J. C. Burant, S. S. Iyengar, J. Tomasi, M. Cossi, N. Rega, J. M. Millam, M. Klene, J. E. Knox, J. B. Cross, V. Bakken, C. Adamo, J. Jaramillo, R. Gomperts, R. E. Stratmann, O. Yazyev, A. J. Austin, R. Cammi, C. Pomelli, J. W. Ochterski, R. L. Martin, K. Morokuma, V. G. Zakrzewski, G. A. Voth, P. Salvador, J. J. Dannenberg, S. Dapprich, A. D. Daniels, O. Farkas, J. B. Foresman, J. V. Ortiz, J. Cioslowski, D. J. Fox, Gaussian, Inc., Wallingford CT, 2009.
- 4 A. D. Becke, *J. Chem. Phys.*, 1993, **98**, 5648.
- 5 C. Lee, W. Yang and R. G. Parr, *Phys. Rev. B*, 1988, **37**, 785–789.
- 6 P. J. Hay and W. R. Wadt, *J. Chem. Phys.*, 1985, **82**, 270–283.
- 7 W. R. Wadt and P. J. Hay, *J. Chem. Phys.*, 1985, **82**, 284–298.
- 8 P. J. Hay and W. R. Wadt, *J. Chem. Phys.*, 1985, **82**, 293–310.
- 9 G. A. Petersson, A. Bennett, T. G. Tensfeldt, M. A. Al-Laham, W. A. Shirley and J. Mantzaris, *J. Chem. Phys.*, 1991, **94**, 6081–6090.
- 10 J. Melorose, R. Perroy and S. Careas, *J. Chem. Phys.*, 1988, **89**, 2193–2218.
- 11 A.-R. Allouche, *J. Comput. Chem.*, 2011, **32**, 174–182.
- 12 N. M. O’Boyle, A. L. Tenderholt and K. M. Langner, *J. Comput. Chem.*, 2008, **29**, 839–845.
- 13 L. Krause, R. Herbst-Irmer, G. M. Sheldrick and D. Stalke, *J. Appl. Crystallogr.*, 2015, **48**, 3–10.
- 14 G. M. Sheldrick, *Acta Crystallogr. A*, 2008, **A64**, 112–122.
- 15 G. M. Sheldrick, *Acta Crystallogr. C*, 2015, **71**, 3–8.
- 16 L. J. Bourhis, O. V Dolomanov, R. J. Gildea, J. A. K. Howard and H. Puschmann, *Acta Crystallogr.*, 2015, **A71**, 7–13.
- 17 H. Benjamin, Y. Zheng, A. S. Batsanov, M. A. Fox, H. A. Al-Attar, A. P. Monkman and M. R. Bryce, *Inorg. Chem.*, 2016, **55**, 8612–8627.
- 18 R. Davidson, Y.-T. Hsu, T. Batchelor, D. Yufit and A. Beeby, *Dalton Trans.*, 2016, **45**, 11496–11507.
- 19 L.-O. Pålsson and A. P. Monkman, *Adv. Mater.*, 2002, **14**, 757–758.
- 20 M. Micksch, M. Tenne and T. Strassner, *Eur. J. Org. Chem.*, 2013, 6137–6145.